Herbivorous insects independently evolved salivary effectors to regulate plant immunity by destabilizing the malectin-LRR RLP NtRLP4

Xin Wang[1,2], Jia-Bao Lu[1], Yi-Zhe Wang[1], Xu-Hong Zhou[3], Jian-Ping Chen[1,2], Chuan-Xi Zhang[1], Jun-Min Li[1,#], Hai-Jian Huang[1,#]

[1] State Key Laboratory for Quality and Safety of Agro-Products, Key Laboratory of Biotechnology in Plant Protection of MARA, Zhejiang Key Laboratory of Green Plant Protection, Institute of Plant Virology, Ningbo University, Ningbo 315211, China

[2] Institute of Applied Ecology, Fujian Agriculture and Forestry University, Fuzhou 350002, China

[3] Office of Science and Technology, Yunnan University of Chinese Medicine, Kunming 650205, China

Abstract

Plants rely on receptor-like proteins and receptor-like kinases (RLPs/RLKs) to detect a variety of invading pathogens and insects. However, it remains unclear how these invaders are able to overcome receptor perception and disable the plant signaling pathways. Here, we show that whiteflies and planthoppers independently evolve salivary effectors to target defensive RLP4, therefore minimizing the plant immunity. RLP4 is a leucine-rich repeat RLP (LRR-RLP) that confers plant resistance against herbivorous insects by forming RLP4/SOBIR1 complexes. In whitefly *Bemisia tabaci*, BtRDP is an Aleyrodidae-restricted protein that attaches to salivary sheath. It interacts with RLP4 from different plants, causing the degradation of RLP4 in an ubiquitin-dependent manner. Transgenic plants overexpressing NtRLP4 exerts a detrimental impact on *B. tabaci* by exploiting the crosstalk between the salicylic acid (SA) and jasmonic acid (JA) pathways. Conversely, the overexpression of BtRDP or silencing of NtRLP4 effectively alleviates such negative effects. In planthopper *Nilaparvata lugens*, a Delphacidae-restricted salivary protein NlSP694 also targets and promotes degradation of OsRLP4 from rice plants. Our results reveal the

* Corresponding authors: Jun-Min Li, lijunmin@nbu.edu.cn; Hai-Jian Huang, huanghaijian@nbu.edu.cn

convergent evolution of salivary proteins in insects, and shed lights on the complex interactions between plants and herbivorous insects.

Keywords

salivary effector, insect-plant interaction, receptor-like protein, convergent evolution

Introduction

The activation of innate immunity by membrane-localized receptors is a highly conserved mechanism in eukaryotes [1]. In sessile plants, the first line of defense against potential pathogenic microbes or insects relies on cell surface pattern-recognition receptors (PRRs) [2]. The plant genome encodes hundreds of PRRs, including receptor-like kinases (RLKs) and receptor-like proteins (RLPs) [2]. RLKs consist of different types of N-terminal ectodomains, a single transmembrane domain, and a cytoplasmic protein kinase domain, while RLPs have a similar structure but lack the kinase domain [3, 4]. As RLPs lack intracellular signaling domains, they are usually associated with SOBIR1 or SOBIR1-like adaptors to form bimolecular receptor kinases [4]. Despite the large number of PRRs encoded by plant genomes, only a few of them have been well characterized in terms of their function in recognizing microbial-associated molecular patterns (MAMPs), damage-associated molecular patterns (DAMPs), and herbivore-associated molecular patterns (HAMPs) [3, 5]. For instance, FLS2 is known to recognize bacterial flagellin [6], EFR can recognize bacterial elongation factor Tu [7], and EIX2 is responsible for recognizing the fungal ethylene-inducing xylanase [8].

Piercing-sucking insects, such as whiteflies, aphids, and planthoppers, damage plants by feeding or transmitting viruses. They inject a mixture of saliva into plant tissues, which aids their performance by binding to the leaked calcium, degrading extracellular DNA, and regulating plant hormonal signals [9-12]. In response, plants have evolved the ability to detect herbivores by sensing HAMPs present in insect saliva [5, 13]. This triggers pattern-triggered immunity (PTI), including mitogen-activated protein kinase (MAPK) cascades, reactive oxygen species (ROS), and hormone signaling [14-16]. Although a few salivary proteins have been reported to activate plant PTI, the specific PRRs that recognize these proteins and trigger plant immunity are still not well understood [17-19]. One exception is the inceptin receptor (INR), which is a legume-specific LRR-RLP

recognizing the Vu-In in insect oral secretions [5]. Moreover, plant PRRs have been widely reported to be targeted by pathogen effectors [20-22]. It remains unknown how insects cope with the immune recognition system.

The whitefly *Bemisia tabaci* (Hemiptera: Aleyrodidae) and brown planthopper *Nilaparvata lugens* (Hemiptera: Delphacidae) are notorious pests globally. During the feeding process, both insects secrete abundant species-specific salivary proteins into host plants [23, 24]. The plants have been reported to initiate defense responses when they recognize insect feeding [17, 25]. However, the specific PRRs responsible for this process are unknown. Both insects can successfully ingest phloem saps with limited plant defenses. It remains unclear how insects attenuate plant defenses. Given that many defense mechanisms are conserved across plants [1, 26], it is interesting to investigate whether insect evolves a similar strategy to aid feeding in convergent evolution. In this study, we characterize the function of RLPs in plant immunity responsive to piercing-sucking insects, and demonstrate that *B. tabaci* and *N. lugens* independently evolve salivary proteins to regulate the posttranslational modification of RLPs.

Results

BtRDP is most abundantly expressed in salivary glands and secreted into host plants

According to the transcriptomic results, BtRDP (*B. tabaci* RLP-degrading protein; GenBank accession: MN738093) is the most abundantly expressed gene in salivary glands [24]. It is a secretory protein containing a signal peptide at the N-terminal, and totally 6 unique peptides from BtRDP are detected in *B. tabaci* watery saliva (Fig. S1). As there is no gene homolog identified in the NCBI nr database, BtRDP is subjected to BLAST analysis against the transcriptomic or genomic data of 30 insect species. The results show that RDP is distributed in all the analyzed Aleyrodidae species, while no RDP homolog is detected in other species (Table S1). Based on phylogenetic analysis, RDPs from five *B. tabaci* cryptic species are clustered in the same clade, showing a close relationship to RDP from *Aleurocanthus spiniferus* (Fig. S2).

BtRDP can be secreted into host plants, with two bands between 25-35kDa being detected in *Nicotiana tabacum* plants infested by *B. tabaci*, but not in the non-infested plants (Fig. 1a). The smaller high intensity band is the same size as that of BtRDP in salivary glands, and always presents in the *B. tabaci*-infested plants. For the larger lower intensity band, it presents in infested samples

88 with lower frequency. It is possible that the larger band might be the BtRDP that undergoes
89 modification after being secreted into plants, similar with another salivary effector previously
90 reported [27]. However, we cannot exclude the possibility that this larger band is the non-specific
91 *N. tabacum* protein induced by *B. tabaci* feeding. Western-blotting, qPCR and transcriptomic
92 analysis demonstrate that BtRDP is nearly exclusively expressed in the salivary glands (Fig. 1b, c;
93 Fig. S3a), which is significantly different from the actin or ribosomal 18S rRNA (Fig. S4a). In
94 addition, BtRDP is mainly expressed in the adult stages, but lowly expressed in the egg, nymph, and
95 pseudopupa stages (Fig. 1d; Fig. S3b), similar to another salivary protein BtFTSP [28] but different
96 from actin or ribosomal 18S rRNA (Fig. S4b). Immunohistochemical (IHC) staining shows that
97 BtRDP is specifically distributed in principle salivary gland, but not in the accessory salivary gland
98 or other tissues (Fig. 1e). A few salivary proteins have been reported to attach to salivary sheath
99 after secretion [29]. We also stain the salivary sheath secreted by *B. tabaci* using anti-BtRDP serum.
100 The results show that BtRDP signal is mainly detected in the protuberant structure of sheath (Fig.
101 S5), indicating that BtRDP attaches to salivary sheath after secretion.
102
103 **BtRDP is important for *B. tabaci* feeding on tobacco plants**
104 RNA interference is firstly employed to investigate the potential role of BtRDP in whitefly
105 feeding, and ds*BtRDP* treatment efficiently and specifically suppresses the target gene at
106 transcriptional and protein level (Fig. 2a; Fig. S6). We do not observe a significant difference in
107 salivary sheath morphology between ds*BtRDP*- and ds*GFP*-treated *B. tabaci* (Fig. S7a). However,
108 the salivary sheath length of ds*BtRDP*-treated *B. tabaci* is significantly shorter than that of the
109 ds*GFP*-treated control (Fig. S7b). Moreover, ds*BtRDP* treatment exerts no influence on the whitefly
110 survivorship (Fig. S7c). For reproduction analysis, the ds*BtRDP*-treated whiteflies oviposit less eggs
111 than the control (Fig. 2b). The whitefly feeding behavior, which can be classified into
112 nonpenetration (np), pathway duration (C), phloem salivation (E1), and phloem ingestion (E2) [30]
113 (Fig. S8), is recorded using the electrical penetration graph (EPG) technique. Compared with ds*GFP*
114 treatment, ds*BtRDP*-treated *B. tabaci* exhibits a dramatic decrease in phloem ingestion (Fig. 2c).
115 Moreover, ds*BtRDP*-treated whitefly exhibits a significantly increased pathway duration phase and
116 a slightly increased nonpenetration phase (Fig. 2c).
117 Salivary proteins are reported to function in intercellular space and/or extracellular space after

118 secreted into host plants [29, 31]. To investigate the role of BtRDP in different subcellular location
119 of host plants, we construct two transgenic *N. tabacum* overexpressing BtRDP, one with a complete
120 coding region (oeBtRDP) and the other without signal peptide (oeBtRDP^{-sp}). The signal peptide of
121 BtRDP may enable protein secretion into the extracellular space. The flag tag is fused to the C-
122 terminal ends of recombinant proteins, respectively. The empty vector (EV) transgenic plants, which
123 exert no significant influence on insect performance compared with the WT (Fig. S9), is used as a
124 negative control. Fecundity assay demonstrates that both oeBtRDP and oeBtRDP^{-sp} transgenic
125 plants are beneficial to whiteflies, with more eggs oviposited in these two overexpressing plants
126 compared with the EV controls (Fig. 2d-i; Fig. S10). Two-choice experiments exert similar results,
127 with more insects being settled and oviposited in oeBtRDP or oeBtRDP^{-sp} transgenic plants than the
128 EV controls (Fig. 2d-i; Fig. S10). These results indicate that BtRDP is beneficial to whiteflies,
129 regardless of its subcellular location in host plants.

130 Transcriptomic sequencing is performed on EV, oeBtRDP#1, and oeBtRDP^{-sp}#1 transgenic
131 plants. PCA analysis demonstrates that the biological replicates of each transgenic plant can be well
132 clustered (Fig. S11a). Totally 1253 and 1227 differentially expressed genes (DEGs) are identified
133 when comparing oeBtRDP#1 and oeBtRDP^{-sp}#1 with EV plants, respectively (Table S2; Table S3).
134 Enrichment analysis of DEGs in these two comparison groups exerts similar results, with pathways
135 associated with MAPK signaling, environmental adaptation, signal transduction, and plant-
136 pathogen interaction significantly enriched (Fig. S10b, c). There are 464 DEGs overlap in these two
137 comparison groups (Fig. S11d). Interestingly, the majority of these DEGs exhibit similar expression
138 pattern in oeBtRDP#1 and oeBtRDP^{-sp}#1 when compared with EV plants (Fig. S11e), suggesting
139 that BtRDP affect some plant pathways regardless of its subcellular location. There are 1084 DEGs
140 identified in comparison of oeBtRDP#1 and oeBtRDP^{-sp}#1 plants (Table S4). Enrichment analysis
141 show that the DEGs associated with metabolism, diterpenoid biosynthesis, and plant-pathogen
142 interaction are significantly enriched (Fig. S12), suggesting that subcellular location of BtRDP also
143 has non-negligible influence on host plants.

144

145 **BtRDP interacts with NtRLP4/NtSORBIR1 complex**

146 To investigate the underlying mechanism of BtRDP in improving whitefly feeding, yeast two-
147 hybrid (Y2H) screening against a *N. benthamiana* cDNA library is conducted using BtRDP^{-sp} as a

148 bait. Totally seven proteins are found to potentially interact with BtRDP^{-sp} (Table S5), including an
149 NbRLP4 (accession Niben261Chr07g1310001.1 in Niben261 genome). NbRLP4 contains a
150 predicted N-terminal signal peptide, a malectin-like domain, a LRR domain, followed by a
151 transmembrane domain. NbRLP4, as well as its closest homology in *N. tabacum* (NtRLP4;
152 GenBank accession: XM_016601109), does not contain the kinase domain (Fig. 3a).

153 The relative expression of *NtRLP4* in response to *B. tabaci* infestation is investigated. qRT-
154 RCR results demonstrate that the transcript level of *NtRLP4* is not significantly influenced by *B.*
155 *tabaci* (Fig. S13). However, a decrease in protein level of NtRLP4 is detected by western-blotting
156 assay (Fig. 3b). Point-to-point Y2H assays reveal that NtRLP4 without signal peptides and
157 transmembrane domains interacts with BtRDP^{-sp} (Fig. 3c). To investigate the specificity of NtRLP4-
158 BtRDP interaction, another RLP protein NtCf9 showing the highest sequence similarity to tomato
159 resistance protein Cf9 [32], as well as three randomly selected salivary proteins from *B. tabaci*, are
160 used as controls. The results show that BtRDP^{-sp} cannot interact with truncated NtCf9 without signal
161 peptides and transmembrane domains (Fig. 3c). Also, NtRLP4$_{(23-541)}$ cannot interact with the other
162 three salivary proteins without signal peptides (Fig. S14a, b). In addition, it is the LRR domain, but
163 not the malectin-like domain or the short intercellular region, that is required for the NtRLP4-BtRDP
164 interaction (Fig. 3c). To investigate the shortest LRR sequence responsible for BtRDP interaction,
165 LRR domain is divided into three segments. However, none of these segments interact with BtRDP-
166 ^{sp} (Fig. S14a). Co-immunoprecipitation (Co-IP) assays further confirm the specific interaction
167 between BtRDP and NtRLP4 (Fig. 3d). It is the C-terminal myc tag-fused NtRLP4 (NtRLP4-myc),
168 but not the NtCf9 (NtCf9-myc), that can be immunoprecipitated by C-terminal flag tag fused BtRDP
169 (BtRDP-flag). In bimolecular fluorescence complementation (BiFC) assay, YFP fluorescence is
170 observed when co-expressing the N-terminal nYFP tag fused NtRLP4 and N-terminal cYFP tag
171 fused BtRDP^{-sp} (Fig. S14c). Furthermore, oeBtRDP transgenic plants that overexpressing BtRDP-
172 flag are incubated with anti-flag beads. The results show that endogenous NtRLP4 can be
173 immunoprecipitated, which is significantly different from the control (Fig. S14d). These results
174 suggest that BtRDP interacts with NtRLP4.

175 The absence of kinase motifs in the C-terminal region of NtRLP4 suggests that it must function
176 in cooperation with other proteins to initiate the signaling. The receptor-like kinase SOBIR1, which
177 contained a kinase domain (Fig. S15a), is reported to be required for the function of several RLPs

178 involved in the innate immunity [4]. Through Co-IP assays, our study demonstrates that NtRLP4 is
179 capable of interacting with NtSOBIR1 (Fig. S15b).
180
181 **NtRLP4 and NtSOBIR1 are resistant to *B. tabaci* infestation**
182 The transgenic *N. tabacum* overexpressing NtRLP4 (oeRLP#1 and oeRLP#2, without any tags)
183 is constructed (Fig. 3e). Compared with the EV control, both oeRLP lines are less attractive to *B.*
184 *tabaci*, with less settling and ovipositing insects (Fig. 3f; Fig. S16a). Also, we observe the
185 significantly decreased fecundity of *B. tabaci* in oeRLP plants (Fig. 3g; Fig. S16b). Similar results
186 are observed after transient overexpression of NtRLP4-GFP in *N. tabacum* (Fig. S16c, d), indicating
187 that NtRLP4 is resistant to *B. tabaci* infestation.
188 Thereafter, the EV and oeRLP#1 plants are subjected to transcriptomic sequencing (Fig. 17a).
189 Totally 729 differentially expressed genes (DEGs) are identified, including 423 up-regulated and
190 306 down-regulated ones (Table S6). Enrichment analysis demonstrate that the majority of up-
191 regulated DEGs are associated with plant-pathogen interaction, environmental adaptation, MAPK
192 signaling pathway, and signal transduction (Fig. 17b). By contrast, the glutathione metabolism,
193 carbohydrate metabolism, and amino acid metabolism pathways are significantly enriched in down-
194 regulated DEGs (Fig. 17c). Noteworthily, there are many DEGs annotated as RLK/RLP or WRKY
195 transcription factor, with the majority of them being significantly upregulated (Fig. S17d, e). These
196 results suggest an increased defense in oeRLP plants. The crosstalk between salicylic acid (SA) and
197 jasmonic acid (JA) pathways is critical for plant defenses [12]. The increased defense of oeRLP
198 transgenic plant is partially caused by the altered hormonal signaling. The JA-associated genes
199 *FAD7* is significantly induced, while the SA-associated genes *PAL* and *NPR1* are repressed in oeRLP
200 plants (Fig. 3h). Transient overexpression of NtRLP4-GFP in *N. tabacum* plants via *Agrobacterium*
201 infiltration exert similar results (Fig. S16e). Furthermore, NtRLP4-GFP significantly enhances the
202 H_2O_2 accumulation (Fig. S16f).
203 We also investigate the function of NtSOBIR1 by transient overexpression and hairpin RNAi (Fig.
204 S18). Overexpression of NtSOBIR1-GFP induces the cell death phenotype five days post agro-
205 injection (Fig. S18b). Insects prefer to settle and oviposit on GFP-expressed *N. tabacum* than on
206 NtSOBIR1-GFP-expressed control, even no obvious death phenotype is observed two days post
207 agro-injection (Fig. S18c, d). For NtSOBIR1 silencing, no cell death phenotype is observed, while

208 the NtSOBIR1-silenced leaves exhibit reduced growth (Fig. S18f). Compared with EV-silenced
209 control, NtSOBIR1-silenced *N. tabacum* is slightly attractive to *B. tabaci* (Fig. S18g, h).
210 Collectively, these results demonstrate that NtSOBIR1 is resistant to *B. tabaci* infestation.
211
212 **BtRDP attenuates plant defenses by promoting the degradation of host RLP4**
213 To investigate the interplay between NtRLP4 and BtRDP, we construct transgenic *N. tabacum*
214 silencing NtRLP4 (*RNAi-RLP*#1 and *RNAi-RLP*#2) (Fig. S19a). Compared with EV plants, *B.*
215 *tabaci* show a tendency to settle on NtRLP4-silenced plants and lay more eggs (Fig. S19b, c).
216 Thereafter, ds*GFP*- and ds*BtRDP*-treated *B. tabaci* are reared on EV, *RNAi-RLP*#1, and *RNAi-*
217 *RLP*#2, respectively. The ds*BtRDP*-treated *B. tabaci* produce less offspring than the control
218 (decreased by 28.3%; P=0.0007) on EV plants (Fig. 4a), consistent with the results on WT plants
219 (Fig. 2b). On *RNAi-RLP*#1 plant, the impair insect reproduction is still observed after ds*BtRDP*
220 treatment, but the extent is slightly reduced (decreased by 23.7%; P=0.002) (Fig. 4a). On *RNAi-*
221 *RLP*#2 plant, there is no statistical significance between ds*GFP* and ds*BtRDP* treatments (Fig. 4a).
222 These results suggest that *RNAi-RLP* plants are beneficial for insects and can partially, but not
223 completely, rescue the impaired feeding performance of ds*BtRDP*-treated insects.
224 To investigate the influence of BtRDP on NtRLP4, the GFP-tagged NtRLP4 (NtRLP4-GFP) is
225 transiently co-expressed with mCherry-tagged BtRDP (BtRDP-mCherry), red fluorescent protein
226 (RFP)-mCherry, and BtFTSP1-mCherry via agroinfiltration, respectively. All tags are fused to the
227 C-terminus. BtRDP-mCherry does not influence the location patterns of NtRLP4-GFP (Fig. S20).
228 However, a significant reduction in the fluorescent signal of NtRLP4-GFP is detected when co-
229 expressed with BtRDP-mCherry, but not the controls (Fig. S20). The co-expression of BtRDP-
230 mCherry/NtRLP4-GFP significantly reduces H_2O_2 accumulation (Fig. 4b) and suppresses the
231 expression of the JA-associated genes *FAD7* and *PDF.12*, while inducing the expression of the SA-
232 associated genes *PAL* and *NPR1* (Fig. 4c). Insect bioassays demonstrate that transient
233 overexpression of BtRDP-mCherry rescues the negative effects on whitefly performance caused by
234 NtRLP4-GFP overexpression (Fig. 4d, e). In host choice experiments, *B. tabaci* display a preference
235 for settling on *N. tabacum* leaves co-expressing BtRDP-mCherry/NtRLP4-GFP over those co-
236 expressing RFP-mCherry/NtRLP4-GFP (Fig. 4d). We observe almost no preference in *B. tabaci*
237 feeding on *N. tabacum* plants co-expressing BtRDP-mCherry/NtRLP4-GFP and plants expressing

238 GFP alone (Fig. S21).

239 The attenuated NtRLP4-GFP fluorescent signal (Fig. S20), along with the observed decrease
240 in the protein level of NtRLP4 during *B. tabaci* infestation (Fig. 3b), leads us to speculate on whether
241 BtRDP influences the accumulation of NtRLP4. To this end, the BtRDP^{-sp}-his and GFP-his proteins
242 are prokaryotic expressed in *Escherichia coli*. Different concentrations of purified BtRDP^{-sp}-his and
243 GFP-his proteins are infiltrated into *N. tabacum* plants overexpressing NtRLP4-myc. Interestingly,
244 the protein level of NtRLP4-myc shows a slight decrease with increasing amounts of BtRDP^{-sp}-his,
245 while no such effect is observed with GFP-his (Fig. S22). Moreover, the BtRDP^{-sp}-his protein does
246 not have significant effect on the accumulation of another RLP NtCf9-like (Fig. S22).

247 Then, we detect the NtRLP4 level in oeBtRDP and oeBtRDP^{-sp} plants. Compared with the EV
248 control, a reduced NtRLP4 abundance is observed in both oeBtRDP#1 and oeBtRDP#2 transgenic
249 lines, but not the oeBtRDP^{-sp} plants (Fig. 4f), suggesting the importance of BtRDP secretion in
250 extracellular space. BtRDP attaches to salivary sheath that localizes in plant apoplast (Fig. S5). The
251 presence of signal peptide promotes the secretion of BtRDP into extracellular space. Therefore, we
252 use the complete coding region of *BtRDP* in subsequent experiments. The NtRLP4-myc and
253 BtRDP-flag are transiently co-expressed in *N. benthamiana* plants through *Agrobacterium*
254 infiltration. The results show that BtRDP-flag significantly decreasing the protein level of NtRLP4-
255 myc, but not the NtCf9-myc (Fig. 4g). qRT-PCR analyses demonstrate that the transcript level of
256 *NtRLP4* remains unchanged (Fig. S23). These findings indicate that the reduction in protein level
257 of NtRLP4 is not caused by transcriptional changes but rather to degradation.

258 The ubiquitin system and autophagy are two major pathways regulating protein degradation
259 [33]. At first, we employ MG132, a 26S proteasome inhibitor known to inhibit the degradation of
260 ubiquitin-conjugated proteins [34]. The results show that MG132 efficiently prevents the
261 degradation of NtRLP4-myc by BtRDP-flag (Fig. 4h). Then, we employ autophagy inhibitor 3-
262 Methyladenine (3-MA) and bafilomycin A1 (BAF) that can block autophagy in plants [35].
263 However, the decreased protein level of NtRLP4-myc is still observed in the presence of 3-MA or
264 BAF (Fig. S24). Additionally, NtRLP4-myc and HA-tagged ubiquitin (HA-UBQ) are co-expressed
265 in *N. benthamiana*. Total proteins are extracted from *N. benthamiana* leaves and then subjected to
266 immunoprecipitation with anti-myc beads. The ubiquitin attached to NtRLP4 is determined by
267 immunoblot using anti-HA antibody. Leaves expressing NtRLP4-myc or UBQ-HA along are used

268 as negative controls. The results show that a strong UBQ signal is detected in the
269 immunoprecipitated product only when NtRLP4-myc and UBQ-HA are co-expressed (Fig. 4i). The
270 molecular weight of UBQ-attached NtRLP4-myc is remarkably larger than NtRLP4-myc itself (Fig.
271 4i). These results suggest that BtRDP promotes NtRLP4 degradation through the ubiquitin system,
272 but not the autophagy pathway.
273
274 **Degrading plant RLP4s by salivary effectors is a common strategy for insects**
275 To investigate the ability of BtRDP to degrade RLPs from other host plants of *B. tabaci*,
276 *Solanum lycopersicum* RLP4 (SlRLP4; GenBank accession: XP_004232910) is selected for
277 analysis. Sequence analysis reveals a similar gene structure between SlRLP4 and NtRLP4 (Fig. S25;
278 Fig. S26a). The interaction between BtRDP and SlRLP4 is confirmed through Y2H and Co-IP
279 assays (Fig. S26b, c). Moreover, we transiently co-express SlRLP4-myc and SlCf9-like-myc with
280 varying concentrations of BtRDP-flag or GUS-flag, with the myc and flag tags fused to the C-
281 terminus. The results show that BtRDP-flag exerts no influence on the accumulation of SlCf9-like-
282 myc protein. By contrast, the protein level of SlRLP4-myc is significantly reduced in the presence
283 of BtRDP-flag (Fig. S26d), indicating the conserved function of BtRDP in *B. tabaci* adaptation to
284 different host plants.
285 BtRDP is an Aleyrodidae-restricted gene that does not have homologues in other species. To
286 explore whether RLP degradation by salivary effectors is conserved among different herbivorous
287 insects, a RLP4 homology from *Oryza sativa* (OsRLP4; GenBank accession: XP_015645303; Fig.
288 5a) and twenty salivary proteins from planthopper species without signal peptides are paired to
289 identify the potential interactions using Y2H assays. As a result, only the salivary protein NlSP694^{-}
290 ^{sp} (GenBank accession: MF278694) interacts with OsRLP4$_{(29-551)}$ (OsRLP4 without signal peptides
291 and transmembrane domains), while the other salivary proteins analyzed do not (Fig. 5b, c; Fig.
292 S27). NlSP694 does not show any sequence or structure similarity to BtRDP (Fig. S28). Based on
293 truncation analysis, NlSP694^{-sp} interacts with both the LRR domain and malectin-like domain of
294 OsRLP4 (Fig. 5c), slightly different from that of the BtRDP-NtRLP4 interaction (Fig. 3c).
295 Considering that both BtRDP and NlSP694 interact with the LRR domain of RLP4, the specific
296 region of LRR domain responsible for NlSP694 binding is further investigated. The LRR domain
297 of OsRLP4 is divided into three segments, in accordance with the LRR domain division in NtRLP4

298 (Fig. S14a). NlSP694^{-sp} interacts with the truncated LRR domain (OsRLP4$_{(480-526)}$) (Fig. 5c). By
299 contrast, none of the truncated LRR domain of NtRLP4 interact with BtRDP^{-sp} (Fig. S14a). These
300 results suggest that the binding sites of salivary proteins to RLP4 may be different between *N. lugens*
301 and *B. tabaci*.

302 NlSP694 is a planthopper-specific salivary protein that is nearly exclusively expressed in
303 salivary glands (Fig. 5d; Fig. S29). The function of NlSP694 or its gene homologs in other
304 planthopper species has not been well investigated previously. Silencing NlSP694 does not impact
305 insect survivorship (Fig. 5e). However, significant reductions in honeydew excretion and impaired
306 fecundity are observed in ds*NlSP694*-treated *N. lugens* (Fig. 5f, g), indicating the importance of
307 NlSP694 in insect feeding.

308 Subsequently, we transiently co-express OsRLP4-myc with a complete coding region of
309 *NlSP694* (C-terminal flag tagged, NlSP694-flag). Another salivary protein NlSP7-flag and NtCf9-
310 myc are used as negative controls. The results demonstrate that NlSP694-flag specifically and
311 significantly decreases the protein level of OsRLP4-myc, which differs significantly from that of
312 the NlSP7-flag (Fig. 5h). Additionally, we demonstrate that NlSP694-flag fails to decrease the
313 protein level of NtCf9-myc (Fig. 5h). These findings suggest that *N. lugens* potentially evolves
314 salivary effectors to target rice RLPs.

315

316 **Discussion**

317 Plants have evolved a complex innate immune system to protect themselves against
318 pathogen/insect invasion, and the cell surface-localized PRRs function on the frontline [2]. To
319 counteract this response, the pathogens have been reported to develop various methods to avoid
320 plant PRR-mediated PTI for their own advantage [36]. However, it remains unknown whether
321 insects take the similar strategy to sabotage plant immunity. In this study, we demonstrate that the
322 RLP4/SOBIR1 complexes confer plant resistance against herbivorous insects. In response, both
323 planthoppers and whiteflies secrete salivary effectors that facilitate the degradation of defensive
324 RLP4, leading to attenuated plant immunity. Our results suggest that manipulation of PRRs may be
325 a conserved strategy for herbivorous insects.

326 PRRs recognize modified-self or non-self patterns and activate a series of immune signaling,
327 which subsequently regulate downstream defense responses and confer plant resistance against

328 invaders [2, 3]. While various insect salivary components have been reported to trigger plant
329 immune responses, the specific PRRs responsible for this process are elusive. Our study
330 demonstrates that RLP4 exerts a significant impact on insect performance by modulating plant
331 hormones and ROS (Fig. 3f-h; Fig. S16-S17), highlighting the critical role of this gene in plant
332 immunity. Nevertheless, the exact ligand for RLP4 remains unknown. It is possible that malectin-
333 LRR receptor RLP4 responds to the DAMPs or HAMPs that are released during insect feeding [37],
334 which deserved further investigation. RLP4 lacks the intracellular kinase domain, and forms
335 bimolecular receptor kinases by interacting with SOBIR1 (Fig. S15). Overexpression of NtRLP4 or
336 NtSOBIR1 enhances insect feeding, while silencing of either gene exerts the opposite effect (Fig.
337 Fig. S16-S19). The association between RLPs and SOBIR1 protein kinases is a structural and
338 functional equivalent to genuine receptor kinases [4]. Therefore, disrupting the stability of the
339 RLP4/SOBIR1 complex can potentially undermine the immune recognition process.

340 As pivotal regulators in immune signaling, PRRs are frequently targeted by multiple pathogens
341 through diverse mechanism. For example, *Pseudomonas syringae* hampered the functionality of
342 receptor complexes by disrupting the ligand-dependent association between receptor-like kinase
343 BAK1 and the flagellin receptor FLS2 [22], while *Phytophthora infestans* fostered alternative
344 splicing of the host RLPKs to enhance infection [21]. PRRs are usually subjected to degradation via
345 post-translational modifications [38]. In plants, the activity and stability of PRRs undergo stringent
346 regulation since excessive activation of PRRs can be detrimental [20, 39]. One prevalent regulatory
347 mechanism involves ubiquitination followed by subsequent degradation mediated by the 26S
348 proteasome [38]. Mounting evidence has demonstrated the exploitation of such mechanisms by
349 bacteria, fungi, viruses, and oomycetes to facilitate PRR degradation [40-43]. Nevertheless, the
350 occurrence of effector-mediated PRR degradation in insects is unreported. Our study reveals that
351 the salivary effectors BtRDP from *B. tabaci* and NlSP694 from *N. lugens* interact with plant RLP4s,
352 leading to their degradation in an ubiquitin-dependent manner (Fig. 4f-i). Notably, BtRDP and
353 NlSP694 share no sequence or structural similarity and lack resemblance to known eukaryotic
354 ubiquitin-ligase domains. Their interaction with RLP4s occurs in the extracellular space (Fig. 3d;
355 Fig. 5c), whereas the ubiquitin-proteasome system primarily functions in the cytosol and nucleus
356 [44]. Furthermore, NtRLP4 reduction is observed only in oeBtRDP transgenic plants, not in
357 oeBtRDP^{-sp} plants (Fig. 4f), suggesting that BtRDP exerts its influence on NtRLP4 in the

358 extracellular space. These findings might exclude the possibility that BtRDP/NlSP694 harbors E3
359 ligase activity that directly ubiquitinates RLP4s in plant cells. It is likely that salivary proteins
360 indirectly influence the post-translational modification of RLP4, increasing its degradation rate,
361 which warrants further investigation.

362 Herbivorous insects use a combination of salivary components to facilitate successful feeding
363 [29]. Previous studies have shown that *B. tabaci* suppresses plant defenses by leveraging SA-JA
364 crosstalk, with the salivary protein Bt56 playing a pivotal role during this process [12]. Bt56 triggers
365 the SA-signaling pathway by directly interacting with a KNOTTED 1-like homeobox transcription
366 factor [12]. This study investigates the effects of another salivary effector, BtRDP, on plant
367 hormones, and finds that it elicits similar effects to Bt56, albeit primarily impacting the signal
368 recognition process (Fig. 3h; Fig. S16e). This leads us to speculate that different salivary effectors
369 from the same insect species might simultaneously target the same signaling pathway to ensure
370 effective immune suppression. Our analysis reveals that BtRDP interacts with other host genes in
371 addition to NtRLP4 (Table S5), and silencing NtRLP4 cannot completely rescue the impaired
372 feeding performance of ds*BtRDP*-treated insects (Fig. 4a). Salivary proteins exert a crucial role in
373 mediating the interactions between herbivores and plants. The dynamic interplay between plants
374 and insects might be highly complex, one salivary protein can target multiple plant pathways, and
375 one plant pathway is influenced by multiple salivary proteins.

376 In conclusion, this study shows that suppressing PRR-mediated plant immunity may be the
377 common strategy for the successful feeding of herbivorous insects. Whiteflies and planthoppers
378 independently evolve salivary effectors that facilitate the degradation of to degrade defensive RLP4
379 of host plants in an ubiquitin-dependent manner, which can therefore disrupt the RLP4/SOBIR1
380 complexes for signal recognition (Fig. 6).

381

382 ## Material and methods

383 ### Insects and plants

384 A colony of *B. tabaci* (cryptic species MED) was originally collected from a soybean field in
385 Suzhou, Anhui Province, China. The insects were subsequently maintained on *N. tabacum* cv. K326
386 plants under controlled laboratory conditions (25 ± 1 °C, 50–70% relative humidity, 16:8 h
387 light:dark photoperiod). For experimental use, *N. benthamiana* and *N. tabacum* plants were grown

388 in a climate-controlled growth chamber (23 ± 1 °C, 16:8 h light: dark cycle).

389

390 **Phylogenetic analysis of RDP**

391 To identify potential RDP homologs across insect species, we performed a BLASTp search using
392 the BtRDP protein sequence as a query against the predicted proteomes of 30 insect species. Hits
393 were filtered using an E-value cutoff of 10^{-5}. The retrieved RDP homologs were aligned using
394 MAFFT (v7.310) with default parameters [45]. To improve alignment quality, we removed
395 ambiguously aligned regions using Gblocks with default settings. The optimal amino acid
396 substitution model (JTT+G) was determined using ModelTest-NG (v0.1.6). Phylogenetic
397 relationships were inferred using maximum likelihood analysis in RAxML (v0.9.0) with 1000
398 bootstrap replicates to assess branch support [46]. The final tree was visualized and annotated using
399 iTOL (https://itol.embl.de/).

400

401 **Preparation of anti-BtRDP and anti-NtRLP4 serum**

402 The coding sequence of BtRDP (excluding the signal peptide) was PCR-amplified and cloned
403 into the pET-28a vector (Novagen) to generate a C-terminal 6×His-tagged fusion protein. The
404 recombinant plasmid was transformed into *Escherichia coli* Transetta (DE3) competent cells
405 (TransGen Biotech, Beijing, China). Protein expression was induced with 0.5 mM isopropyl-β-D-
406 thiogalactoside (IPTG) at 28°C for 8 h. Bacterial cells were harvested by centrifugation and lysed
407 via ultrasonication for 30 min. The recombinant BtRDP^{-sp}-His protein was purified under native
408 conditions using Ni-NTA agarose (Qiagen, Hilden, Germany) according to the manufacturer's
409 protocol.

410 Purified BtRDP^{-sp}-His protein was used to immunize rabbits (Hua'an Biotechnology,
411 Hangzhou, China) for custom polyclonal antibody production. The anti-NtRLP4 serum, prepared
412 by immunizing rabbits with peptide GQNSDRPISTKNST, was produced via the custom service of
413 Genscript Biotechnology Company (Nanjing, China). The anti-BtRDP serum was subsequently
414 conjugated to Alexa Fluor™ 488 NHS Ester (#A20000, Thermo Fisher Scientific) following
415 standard labeling protocols.

416 The specificity of anti-BtRDP serum was tested by comparing ds*GFP*- and ds*BtRDP*-treated
417 *Bemisia tabaci*. The results showed that ds*BtRDP* significantly reduced the target gene. Similarly,

418 the specificity of anti-NtRLP4 serum was tested by comparing RNAi-EV and RNAi-NtRLP4 plants,
419 which showed a reduced NtRLP4 expression in *RNAi-NtRLP4* plants.
420
421 **Immunohistochemistry (IHC) staining**
422 Dissected *B. tabaci* heads with attached salivary glands and Parafilm-embedded salivary
423 sheaths were fixed in 4% paraformaldehyde (#E672002, Sango Biotechnology, Shanghai) for 30
424 min. Salivary sheaths adherent to Parafilm were similarly excised and fixed under identical
425 conditions. After fixation, samples were washed three times with PBST (PBS containing 0.1%
426 Tween-20) and blocked with 10% FBS for 2 h at room temperature. The tissues were then incubated
427 overnight at 4°C with Alexa Fluor 488-conjugated anti-BtRDP serum (1:200 dilution), followed by
428 co-staining with phalloidin-rhodamine (1:500, Thermo Fisher Scientific) for 30 min and 4',6-
429 diamidino-2-phenylindole (DAPI) solution (#ab104139, Abcam, Cambridge, USA) for nuclear
430 visualization. Fluorescent images were acquired using a Leica SP8 confocal microscope (Leica
431 Microsystems) to examine BtRDP localization patterns
432
433 **Protein extraction and Western-blotting assays**
434 To identify secreted salivary proteins in *N. tabacum* plants, approximately 200 *B. tabaci* adults
435 were confined in a 3-cm diameter feeding cage and allowed to feed on host plants for 24 h.
436 Following feeding, the infested tobacco leaves were collected, immediately frozen in liquid nitrogen,
437 and ground to a fine powder. The powdered tissue was then homogenized in RIPA Lysis Buffer
438 (#89900, Thermo Fisher Scientific) for protein extraction. To examine the effects of insect feeding
439 on NtRLP expression, groups of approximately 200 *B. tabaci* were allowed to feed on 4-5 true-leaf
440 stage tobacco plants for 12, 24, or 48 h, with uninfested plants serving as controls. For
441 silencing/overexpression efficiency tests, leaf samples were collected at 48 h post-*Agrobacterium*
442 infiltration, along with transgenic tobacco plants at the 4-5 true-leaf stage. For insect tissue analysis,
443 various *B. tabaci* organs were carefully dissected in 1×PBS buffer, including carcasses (20), fat
444 bodies (20), guts (40), salivary glands (60), and ovaries (10), with sample sizes indicated in
445 parentheses. All dissected tissues were transferred to lysis buffer for protein extraction. Total protein
446 concentrations in both insect and plant homogenates were quantified using a BCA Protein Assay
447 Kit (#CW0014S, CwBiotech, Taizhou, China). Equal protein amounts were separated by SDS-

448 PAGE and electro-transferred to PVDF membranes.

449 Membranes were probed with the following primary antibodies: anti-FLAG (1:10,000, #MA1-
450 91878, Thermo Fisher Scientific), anti-MYC (1:10,000, #MA1-21316, Thermo Fisher Scientific),
451 anti-GFP (1:10,000, #MA5-15256, Thermo Fisher Scientific), anti-NtRLP4 (1:5,000, GenScript
452 Biotechnology, Nanjing, China), and anti-BtRDP serum (1:5,000, Huaan Biotechnology, Hangzhou,
453 China). Following primary antibody incubation, membranes were treated with HRP-conjugated
454 secondary antibodies: goat anti-mouse IgG (1:10,000, #31430, Thermo Fisher Scientific) or goat
455 anti-rabbit IgG (1:10,000, #31460, Thermo Fisher Scientific). Protein bands were visualized using
456 an AI 680 image analyzer (Amersham Pharmacia Biotech, Buckinghamshire, UK), with Ponceau S
457 staining used to verify equal protein loading.

458

459 **Quantitative real-time PCR (qRT-PCR) analysis**

460 To prepare tissue-specific samples from *B. tabaci*, adult females were dissected to isolate
461 carcasses (10), fat bodies (10), guts (20), salivary glands (40), and ovaries (10). Additionally,
462 different developmental stages, including eggs (50), nymphs (20), pupae (20), and adult males (20)
463 and females (20), were collected for analysis. The number of insects in each sample is indicated in
464 parentheses. To extract RNA from *N. tabacum* plants, the samples were grinded using liquid
465 nitrogen after collection. Total RNA was extracted using the TRIzol Total RNA Isolation Kit (#9109,
466 Takara, Dalian, China) following the manufacturer's instructions. RNA purity and concentration
467 were assessed using a NanoDrop spectrophotometer (Thermo Fisher Scientific). First-strand cDNA
468 was synthesized from equal amounts of RNA (1 μg) using the HiScript II Q RT SuperMix (#R212-
469 01, Vazyme, Nanjing, China). Gene expression analysis was performed using a Roche LightCycler®
470 480 system (Roche Diagnostics, Mannheim, Germany) with SYBR Green Supermix (#11202ES08,
471 Yeasen, Shanghai, China). The thermal cycling protocol consisted of initial denaturation at 95°C for
472 5 min, and amplification for 40 cycles of 95°C for 10 s and 60°C for 30 s. Primers were designed
473 with Primer Premier v6.0 (Table S7). *B. tabaci Tubulin* and *N. tabacum Tubulin* served as internal
474 controls for normalization. Relative gene expression was calculated using the $2^{-\Delta\Delta Ct}$ method [47].
475 Three to six independent biological replicates, each repeated twice, were performed.

476

477 **RNA interference**

478 The target gene DNA sequences were amplified using primers listed in Table S7 and
479 subsequently cloned into the pClone007 Vector (#TSV-007, Tsingke Biotechnology, Beijing, China).
480 For dsRNA production, PCR-generated DNA templates containing T7 promoter sequences were
481 transcribed *in vitro* using the T7 High Yield RNA Transcription Kit (#TR101-01, Vazyme Biotech,
482 Nanjing, China). The RNAi experiments were performed according to established methods [48].
483 Briefly, newly emerged adult whiteflies were anesthetized with carbon dioxide for 5-10 seconds.
484 Approximately 50 nL of dsRNA solution (2 μg/μL) was microinjected into the mesothorax of each
485 insect using a FemtoJet microinjection system (Eppendorf, Hamburg, Germany). Following
486 injection, the whiteflies were maintained on healthy *N. tabacum* leaves under standard rearing
487 conditions. Only actively moving insects were selected for subsequent analyses. Gene silencing
488 efficiency was evaluated on day 4 post-injection using both qRT-PCR and Western-blotting
489 approaches.
490
491 **Generation of transgenic plants**
492 We generated two transgenic *N. tabacum* lines expressing different BtRDP variants: one
493 containing the full coding sequence (oeBtRDP) and another lacking the signal peptide (oeBtRDP^{-}
494 ^{sp}), which may affect protein secretion. The target sequences, along with the full-length NtRLP4
495 coding sequence and an NtRLP4 hairpin RNAi construct, were each cloned into the pBWA(V)HS
496 vector with C-terminal FLAG tags. All constructs were transformed into *A. tumefaciens* strain
497 GV3101 and used to generate transgenic tobacco plants (K326 background) through
498 *Agrobacterium*-mediated transformation performed by Wuhan Boyuan Biological Company.
499 Transgenic lines were verified by qRT-PCR and western blotting, with empty vector-transformed
500 plants serving as controls, and two independent lines for each construct were selected for further
501 experiments.
502
503 **Target gene silencing in plants**
504 The hairpin RNAi construct targeting *NtSOBIR1* was generated by cloning the specific
505 fragment into the pBWA(V)HS plasmid using BsaI and Eco31I restriction enzymes. The
506 recombinant vector was then transformed into *A. tumefaciens* strain GV3101 and subsequently
507 infiltrated into *N. tabacum* leaves using the agroinfiltration method. Following a 48-h incubation

508 period under standard growth conditions, silencing efficiency was quantitatively evaluated by qRT-
509 PCR analysis.
510
511 **Transcriptomic sequencing**
512 To investigate the transcriptional effects of NtRLP4, BtRDP, and BtRDP^{-sp} in *N. tabacum*, leaf
513 samples from EV, oeRLP4#1, oeBtRDP#1, and oeBtRDP^{-sp}#1 transgenic plants were homogenized
514 in TRIzol Reagent (#10296018, Invitrogen, Carlsbad, CA, USA) for total RNA extraction following
515 the manufacturer's protocol. Afterwards, total RNA was extracted according to the instructions of
516 the manufacturer, and the RNA samples were sent to Novogene Institute (Novogene, Beijing, China)
517 for transcriptomic sequencing. Briefly, poly(A)+ RNA was isolated from 20 μg pooled total RNA
518 using oligo(dT) magnetic beads, followed by fragmentation in divalent cation buffer at 94°C for 5
519 min. First-strand cDNA synthesis was performed using N6 random primers, with subsequent
520 second-strand synthesis to generate double-stranded cDNA. After end-repair and Illumina adapter
521 ligation, the products were PCR-amplified (15 cycles) and purified using a QIAquick PCR
522 Purification Kit (#28104, Qiagen, Hilden, Germany). The resulting cDNA libraries were quantified
523 and quality-checked before paired-end sequencing on an Illumina NovaSeq 6000 platform. All raw
524 sequencing data were deposited in the National Genomics Data Center under accession number
525 PRJCA025907.
526
527 **Analysis of transcriptomic data**
528 The raw sequencing reads were quality-filtered using Illumina's internal software, and the
529 resulting clean reads from each cDNA library were aligned to the *N. tabacum* reference genome in
530 Sol Genomics Network
531 (https://solgenomics.net/ftp/genomes/Nicotiana_tabacum/edwards_et_al_2017/) using HISAT
532 v2.1.0 [49]. Low-quality alignments were removed using SAMtools (v1.7) with default parameters
533 [50]. Transcript abundance was quantified as Transcripts Per Million (TPM) using Cufflinks (v2.2.1)
534 [51]. Differential expression analysis was performed with DESeq2 (v2.2.1) [52], identifying
535 significantly DEGs using thresholds of |log2(fold change)| > 1 and adjusted p-value < 0.05. PCA of
536 transcriptome profiles was conducted using a custom R script plotPCA (github.com/franco-
537 ye/TestRepository/blob/main/PCA_by_deseq2.R). For functional annotation, KEGG pathway

538 enrichment analysis was performed in TBtools (v2.083) using a one-sided hypergeometric test:
539 $P = 1 - \sum_{i=0}^{m-1} \left(\frac{\binom{M}{i}\binom{N-M}{n-i}}{\binom{N}{n}} \right)$, [53]. In this software, enriched *P*-values were calculated according to
540 one-sided hypergeometric test: with *N* representing the number of gene with KEGG annotation, *n*
541 standing for the number of DEGs in *N*, *M* indicating the number of genes in each KEGG term, and
542 *m* suggesting the number of DEGs in each KEGG term.
543
544 **Insect bioassays**
545 To survivorship analysis, newly emerged *B. tabaci* adults were microinjected with dsRNA and
546 placed on *N. tabacum* leaves. After 24 h, any dead individuals (potentially due to injection injury)
547 were removed. For each treatment, 20-30 surviving adults were transferred to leaf cages, and
548 mortality was recorded daily for 10 days. Three independent biological replications were performed.
549 For fecundity analysis, dsRNA-treated virgin females were paired with untreated males in
550 leaf cages. Five such pairs were maintained per cage (n=10-12 cages per treatment). Egg deposition
551 was quantified daily for 3 consecutive days under controlled conditions. Each male-female pair was
552 considered an experimental replicate.
553 For host preference test, detached *N. tabacum* leaves with moist cotton-wrapped petioles were
554 arranged in a 50-cm diameter choice arena with a central release chamber. Forty adult whiteflies
555 were released per chamber, and settling preference was recorded at 3, 6, 12, 24, 36, and 48 h post-
556 release. The experiment included 10-12 replicates per treatment, with leaf positions randomized
557 between replicates to eliminate positional bias.
558
559 **EPG recording and analysis**
560 Feeding behavior of *B. tabaci* was monitored using a GiGA-8d EPG amplifier (Wageningen
561 Agricultural University; 10 TΩ input resistance, <1 pA input bias current) with 50× gain and ±5 V
562 output range. Prior to recording, dsRNA-treated whiteflies were starved for 12 h on moist filter
563 paper, briefly anesthetized with CO_2 (10 s), and connected to the amplifier via a gold wire electrode
564 (20 μm diameter × 5 cm length) attached to the pronotum using conductive silver glue. Plant
565 electrodes consisted of copper wires (2 mm diameter × 10 cm length) inserted into the soil of potted
566 *N. tabacum*. Recordings were conducted for 8 h in a Faraday cage (120×75×67 cm; Dianjiang,

567 Shanghai), with only insects surviving the full duration retained for analysis.

568 Recorded waveforms were processed using PROBE 3.4 software (Wageningen Agricultural
569 University) and categorized into four distinct feeding phases: nonpenetration (np), pathway duration
570 (C), phloem salivation (E1), and phloem ingestion (E2) as defined in a previous study [30]. Each
571 treatment included ⩾10 biological replicates, with ds*GFP*-injected and untreated whiteflies
572 serving as controls.

573

574 ***Agrobacterium*-mediated plant transformation in *N. tabacum* and *N. benthamiana***

575 The recombinant expression vectors were introduced into *A. tumefaciens* strain GV3101 via
576 heat shock transformation. Transformed cells were selected on LB agar plates supplemented with
577 50 μg/mL kanamycin and 10 μg/mL rifampicin, followed by incubation at 28°C for 60 h. Positive
578 colonies were inoculated into liquid LB medium with the same antibiotics and grown to log phase.
579 Bacterial cells were then pelleted by centrifugation at 2,400 *g* for 2 min and resuspended in induction
580 buffer (10 mM $MgCl_2$, 10 mM MES [pH 5.6], 200 μM acetosyringone) adjusted to specific OD_{600}
581 values depending on the experiment.

582 For standard experiments, bacterial suspensions were normalized to OD_{600} = 1.0, while
583 degradation assays used three concentrations (OD_{600} = 0.05, 0.3, and 1.0). Equal volumes of selected
584 bacterial suspensions were mixed and infiltrated into leaves of 4–5-week-old *N. tabacum* and *N.*
585 *benthamiana* plants using a needleless syringe. Infiltrated plants were maintained under controlled
586 conditions for subsequent analysis.

587

588 **Diaminobenzidine (DAB) staining**

589 To detect H_2O_2 accumulation in *N. tabacum* leaves, leaf samples were immersed in 1 mg/mL
590 3,3'-diaminobenzidine tetrahydrochloride (DAB-HCl, #D8001, Sigma-Aldrich, St. Louis, MO,
591 USA) solution (pH 3.8) for 6 hours at room temperature, allowing H_2O_2-dependent brown
592 polymerization to occur. Following incubation, the DAB solution was replaced with 100% ethanol
593 for chlorophyll removal, and samples were decolorized overnight at 65°C. The destained leaves
594 were then photographed under standardized conditions using a Canon EOS 80D digital camera
595 (Canon Inc., Tokyo, Japan).

596

597 **Interaction assays between two proteins**

598 In the Y2H screening assay, the coding sequence of BtRDP^{-sp} was cloned into the pGBKT7
599 bait vector (Clontech, USA), while a *N. benthamiana* cDNA library was constructed in the pGADT7
600 prey vector (Biogene Biotech, Shanghai, China). These recombinant vectors were co-transformed
601 into yeast strain Y2HGold and plated on QDO medium (SD/-Ade/-His/-Leu/-Trp, #630428, Takara)
602 for 3 days at 30°C. Positive colonies were cultured in QDO liquid medium, and plasmids were
603 extracted using a yeast DNA kit (#DP112-02, TIANGEN, Beijing, China) before transformation
604 into E. coli DH5α (#TSC-C14, Tsingke) for sequencing (YouKang Biotech, China) to identify
605 interacting partners.

606 In the Y2H point-to-point verification assay, BtRDP^{-sp} and NlSP694^{-sp}, and mutant variants of
607 NtRLP4/SlRLP4/ OsRLP4 were cloned into either pGBKT7 or pGADT7 vectors using primers
608 from Table S7. Yeast co-transformants were first selected on DDO medium (SD/-Leu/-Trp)
609 (#630417, Takara) for 3 days at 30°C, then spotted onto QDO medium to confirm interactions
610 through growth after another 3 days of incubation.

611 In the Co-IP assays, Full-length sequences of *BtRDP*, *NlSP694*, *NtSOBIR1*, *NtRLP4*, *SlRLP4*,
612 and *OsRLP4* were cloned into lic-myc or lic-flag vectors for C-terminal tagging, with BtFTSP-flag
613 serving as a negative control. Five-week-old *N. benthamiana* leaves were agroinfiltrated with these
614 constructs or collected from oeBtRDP transgenic plants. Total proteins were extracted from 1 g
615 frozen tissue in IP lysis buffer (#87788, Thermo Scientific) with protease inhibitors (#56079200,
616 Roche, Switzerland), followed by centrifugation at 1,000 × *g* for 20 min. Cleared lysates were
617 incubated with anti-flag beads (#L00432-1, GenScript, Nanjing, China) for 4 h at 4°C, washed with
618 PBS, and eluted in 2× SDS-PAGE buffer (500 mM Tris-HCl, pH=6.8, 50% glycerin, 10% SDS,
619 1% bromophenol blue, and 2% β-mercaptoethanol) for Western-blotting assay.

620 In the BiFC assay, BtRDP^{-sp}, BtFTSP^{-sp}, NtRLP4, and NtCf9-like were cloned into the pCV-
621 cYFP or pCV-nYFP vectors, respectively. After transforming *A. tumefaciens* GV3101, pairwise
622 combinations were co-infiltrated into *N. benthamiana* leaves. Following 36-48 h incubation in a
623 growth chamber, reconstituted YFP fluorescence was visualized using a Leica SP8 confocal
624 microscope with standard filter sets for YFP detection.

625

626 **RLP degradation by salivary effectors among different herbivorous insects**

627 To examine salivary protein effects on RLPs, we co-infiltrated *A. tumefaciens* GV3101 strains
628 carrying various constructs into *N. benthamiana* leaves. The recombinant vectors expressed C-
629 terminally tagged proteins: BtRDP-flag, NlSP694-flag, GUS-flag, NlSP7-flag, and myc-tagged
630 RLPs (NtRLP4, SlRLP4, OsRLP4, SlCf9, NtCf9). Bacterial suspensions were mixed at
631 predetermined OD_{600} ratios before infiltration, with leaf samples collected 48 hours post-infiltration
632 for subsequent analysis.

633 For confocal microscopy studies, *N. benthamiana* leaves were co-infiltrated with *A.*
634 *tumefaciens carrying*: (1) NtRLP4-GFP plus BtRDP-mCherry, (2) NtRLP4-GFP plus RFP-mCherry,
635 or (3) NtRLP4-GFP plus BtFTSP-mCherry. The samples were imaged by confocal microscopy at
636 48 h post injection. The same parameters were used in photographing.

637 This study also conducted a treatment on *N. benthamiana* plants that were overexpressing
638 NtRLP4-myc using purified proteins. Briefly, the $BtRDP^{-sp}$ and GFP coding sequences were cloned
639 into pET-28a for 6×His-tagged expression in *E. coli* Transetta (TransGen Biotech). Protein
640 expression was induced with 0.5 mM IPTG at 25°C for 8 h, followed by purification using Ni-NTA
641 agarose and buffer exchange into PBS using a 3-kDa molecular-weight cutoff Amicon Ultra-4
642 Centrifugal Filter Device (Millipore, MA, USA). Different concentrations of purified proteins were
643 infiltrated into leaves of *N. benthamiana* plants stably expressing NtRLP4-myc, with samples
644 collected 24 h post-treatment.

645 To investigate degradation pathways, we infiltrated *N. benthamiana* leaves with: 50 μM
646 MG132 (#M7449, Sigma-Aldrich, Steinheim, Germany), 5 μM 3-MA (#M9281, Sigma-Aldrich,),
647 or 10 nM BAF (#BML-CM110-0100, Enzo Life Sciences, Farmingdale, USA) at 24 h post-
648 agroinfiltration. The samples were incubated for additional24 h. Protein levels were detected using
649 Western-blotting assay.

650

651 ***In planta* ubiquitination assay**

652 Ubiquitination detection in *N. benthamiana* was performed according to the methods
653 previously reported [54]. The recombinant vector for transient expression of the HA-fused ubiquitin
654 protein was kindly provided by Dr. Chao Zheng (Ningbo University). Myc-tagged proteins were co-
655 expressed with HA-UBQ by agroinfiltration, and 50 μM MG132 was injected into the *N.*
656 *benthamiana* leaves one day post *A. tumefaciens* infiltration. Immunoprecipitation was performed

using anti-myc beads (ytma-20, ChromoTek , Planegg-Martinsried, Germany). Ubiquitination signals were detected by immunoblot with anti-HA antibody (HT301, TransGen Biotech, Beijing, China).

Scanning electron microscopy (SEM)

B. tabaci adults were allowed to feed on artificial diet solutions for 24 h. Parafilm sections containing salivary sheaths were carefully excised and rinsed with 1× PBS (pH 7.4) to remove residual diet. The samples were mounted on aluminum stubs, desiccated under vacuum, and sputter-coated with gold before imaging with a TM4000 II Plus SEM (Hitachi, Tokyo, Japan). Salivary sheath length (from apex to base) was measured, with 20 sheaths analyzed per treatment to ensure statistical reliability.

Statistical analysis

The log-rank test (SPSS Statistics 19, Chicago, IL, USA) was used to determine the statistical significance of survival distributions. Two-tailed unpaired Student's *t*-test (comparisons between two groups) or one-way ANOVA test followed by Tukey's multiple comparisons test (comparisons among three groups) was used to analyze the results of qRT-PCR, fecundity analysis, and host choice analysis. The EPG data were first checked for the normality and homogeneity of variance, and those not fitting a normal distribution were $\log_{10}$ transformed before Student's *t* test, as described in previous studies [30]. Data were graphed in GraphPad Prism 9.

Data availability

All data is included in the manuscript and/or supporting information. The transcriptomic data have been submitted to the National Genomics Data Center under accession number PRJCA025907. The original blot images have been displayed in Fig. S30-S33.

References

1. Nürnberger T, Brunner F, Kemmerling B, & Piater L (2004) Innate immunity in plants and animals: striking similarities and obvious differences. *Immunol Rev* 198(1):249-266.
2. Macho AP & Zipfel C (2014) Plant PRRs and the activation of innate immune signaling. *Mol*

687 *Cell* 54(2):263-272.
688 3. Zipfel C (2014) Plant pattern-recognition receptors. *Trends Immunol* 35(7):345-351.
689 4. Gust AA & Felix G (2014) Receptor like proteins associate with SOBIR1-type of adaptors to
690 form bimolecular receptor kinases. *Curr Opin Plant Biol* 21:104-111.
691 5. Adam D. Steinbrennera, *et al.* (2020) A receptor-like protein mediates plant immune responses
692 to herbivore-associated molecular patterns. *Proc Natl Acad Sci USA* 117(49):31510-31518.
693 6. Chinchilla D, Bauer Z, Regenass M, Boller T, & Felix G (2005) The *Arabidopsis* receptor kinase
694 FLS2 binds flg22 and determines the specificity of flagellin perception. *Plant Cell* 18(2):465-
695 476.
696 7. Zipfel C, *et al.* (2006) Perception of the bacterial PAMP EF-Tu by the receptor EFR restricts
697 *Agrobacterium*-mediated transformation. *Cell* 125(4):749-760.
698 8. Ron M & Avni A (2004) The receptor for the fungal elicitor ethylene-inducing xylanase is a
699 member of a resistance-like gene family in tomato. *Plant Cell* 16(6):1604-1615.
700 9. Tian T, *et al.* (2021) A salivary calcium-binding protein from *Laodelphax striatellus* acts as an
701 effector that suppresses defense in rice. *Pest Manag Sci* 77(5): 2272-2281.
702 10. Huang HJ, *et al.* (2019) Salivary DNase II from *Laodelphax striatellus* acts as an effector that
703 suppresses plant defence. *New Phytol* 224(2):860-874.
704 11. Chen CY, *et al.* (2019) An effector from cotton bollworm oral secretion impairs host plant
705 defense signaling. *Proc Natl Acad Sci USA* 116(28):14331-14338.
706 12. Xu HX, *et al.* (2019) A salivary effector enables whitefly to feed on host plants by eliciting
707 salicylic acid-signaling pathway. *Proc Natl Acad Sci USA* 116(2):490-495.
708 13. Chen CY & Mao YB (2020) Research advances in plant-insect molecular interaction. *F1000Res*
709 9(F1000 Faculty Rev):198.
710 14. Guiguet A, *et al.* (2016) Shared weapons of blood- and plant-feeding insects: Surprising
711 commonalities for manipulating hosts. *J Insect Physiol* 84:4-21.
712 15. Wu J & Baldwin IT (2009) Herbivory-induced signalling in plants: perception and action. *Plant*
713 *Cell Environ* 32(9):1161-1174.
714 16. Jiang YJ, Zhang CX, Chen RZ, & He SY (2019) Challenging battles of plants with phloem-
715 feeding insects and prokaryotic pathogens. *Proc Natl Acad Sci USA* 116(47):23390-23397.
716 17. Gao H，*et al*. (2023) The salivary chaperone protein NlDNAJB9 of *Nilaparvata lugens* activated

717 plant immune responses. *J Exp Bot* 74(21):6874-6888.
718 18. Guo H, *et al*. (2020) An aphid-secreted salivary protease activates plant defense in phloem. *Curr*
719 *Biol* 30(24): 4826-4836.
720 19. Bos JI, *et al*. (2010) A functional genomics approach identifies candidate effectors from the
721 aphid species *Myzus persicae* (green peach aphid). *PLoS Genet* 6(11):e1001216.
722 20. Zhang Y & Zeng L (2020) Crosstalk between ubiquitination and other post-translational protein
723 modifications in plant immunity. *Plant Commun* 1(4):100041.
724 21. Huang J*, et al.* (2020) *Phytophthora* effectors modulate genome-wide alternative splicing of
725 host mRNAs to reprogram plant immunity. *Mol Plant* 13(10):1470-1484.
726 22. Shan L*, et al.* (2008) Bacterial effectors target the common signaling partner BAK1 to disrupt
727 multiple MAMP receptor-signaling complexes and impede plant immunity. *Cell Host Microbe*
728 4(1):17-27.
729 23. Huang HJ*, et al.* (2016) Screening and functional analyses of *Nilaparvata lugens* salivary
730 proteome. *J Proteome Res* 15(6):1883-1896.
731 24. Huang HJ, *et al.* (2021) Identification of salivary proteins in the whitefly *Bemisia tabaci* by
732 transcriptomic and LC-MS/MS analyses. *Insect Sci* 28(5):1369-1381.
733 25. Gao H, *et al*. (2022) *Nilaparvata lugens* salivary protein NlG14 triggered defense response in
734 plants. *J Exp Bot* 73(22):7477-7487.
735 26. Mukhtar M, *et al*. (2011) Independently evolved virulence effectors converge onto hubs in a
736 plant immune system network. *Science* 333(6042):596-601.
737 27. Huang J, *et al.* (2020) Salivary protein 1 of brown planthopper is required for survival and
738 induces immunity response in plants. *Front Plant Sci* 11:571280.
739 28. Wang Y, *et al*. (2023) Horizontally transferred salivary protein promotes insect feeding by
740 suppressing ferredoxin-mediated plant defenses. *Mol Biol Evol* 40(10):msad221.
741 29. Huang HJ*, et al.* (2023) Planthopper salivary sheath protein LsSP1 contributes to manipulation
742 of rice plant defenses. *Nat Commun* 14(1):737.
743 30. Lu S, *et al*. (2021) EPG-recorded feeding behaviors reveal adaptability and competitiveness in
744 two species of *Bemisia tabaci* (Hemiptera: Aleyrodidae). *J Insect Behav* 34: 26-40.
745 31. Yan ZW, *et al.* (2023) Endocytosis-mediated entry of a caterpillar effector into plants is
746 countered by Jasmonate. *Nat Commun* 14(1):6551.

747 32. Jones DA, *et al*. (1994) Isolation of the tomato Cf-9 gene for resistance to *Cladosporium fulvum*
748 by transposon tagging. *Science* 266 (5186): 789-793 (1994).
749 33. Varshavsky A, *et al*. (2017) The ubiquitin system, autophagy, and regulated protein degradation.
750 *Annu Rev Biochem* 86: 123-128.
751 34. Li L*, et al.* (2022) Independently evolved viral effectors convergently suppress DELLA protein
752 SLR1-mediated broad-spectrum antiviral immunity in rice. *Nature Commun* 13(1):6920.
753 35. Takatsuka C*, et al.* (2004) 3-Methyladenine inhibits autophagy in tobacco culture cells under
754 sucrose starvation conditions. *Plant Cell Physiol* 45: 265-274.
755 36. Tariqjaveed M*, et al.* (2021) Versatile effectors of phytopathogenic fungi target host immunity.
756 *J Integr Plant Biol* 63(11):1856-1873.
757 37. Doblas VG, *et al.* (2018) Cell wall integrity signaling in plants: Malectin-domain kinases and
758 lessons from other kingdoms. *Cell Surf* 3:1-11.
759 38. Li B, Lu D, & Shan L (2014) Ubiquitination of pattern recognition receptors in plant innate
760 immunity. *Mol Plant Pathol* 15(7):737-746.
761 39. Chen Y, Song Y, Liu J, Xu G, & Dou D (2022) Ubiquitination of receptorsomes, frontline of
762 plant immunity. *Int J Mol Sci* 23(6):2937.
763 40. Langin G, González-Fuente M, & Üstün S (2023) The plant ubiquitin–proteasome system as a
764 target for microbial manipulation. *Annu Rev Phytopathol* 61:351-375.
765 41. Rosas-Diaz T*, et al.* (2018) A virus-targeted plant receptor-like kinase promotes cell-to-cell
766 spread of RNAi. *Proc Natl Acad Sci USA* 115(6):1388-1393.
767 42. Irieda H*, et al.* (2019) Conserved fungal effector suppresses PAMP-triggered immunity by
768 targeting plant immune kinases. *Proc Natl Acad Sci USA* 116(2):496-505.
769 43. Qin J*, et al.* (2018) The Xanthomonas effector XopK harbours E3 ubiquitin-ligase activity that
770 is required for virulence. *New Phytol* 220(1):219-231.
771 44. Xu FQ, Xue HW (2019) The ubiquitin-proteasome system in plant responses to environments.
772 *Plant Cell Environ* 42(10):2931-2944.
773 45. Katoh K & Standley DM (2013) MAFFT multiple sequence alignment software version 7:
774 improvements in performance and usability. *Mol Biol Evol* 30(4):772-780.
775 46. Kozlov AM, Darriba D, Flouri T, Morel B, & Stamatakis A (2019) RAxML-NG: a fast, scalable
776 and user-friendly tool for maximum likelihood phylogenetic inference. *Bioinformatics*

35(21):4453-4455.

47. Livak, K.J., and Schmittgen, T.D. (2001). Analysis of relative gene expression data using real-time quantitative PCR and the $2^{-\Delta\Delta CT}$ method. *Methods* 25, 402-408.

48. Xu HJ*, et al.* (2015) Two insulin receptors determine alternative wing morphs in planthoppers. *Nature* 519(7544):464-467.

49. Kim, D., Langmead, B., and Salzberg, S.L. (2015). HISAT: A fast spliced aligner with low memory requirements. *Nature Methods* 519(7544):464-467.

50. Li, H. (2009). The Sequence Alignment/Map format and SAMtools. *BIOINFORMATICS - OXFORD*.

51. Trapnell, C., Roberts, A., Goff, L., Pertea, G., Kim, D., Kelley, D.R., Pimentel, H., Salzberg, S.L., Rinn, J.L., and Pachter, L. (2012). Differential gene and transcript expression analysis of RNA-seq experiments with TopHat and Cufflinks. *Nature Protocols* 7, 562-578.

52. Wang, L., Feng, Z., Wang, X., Wang, X., and Zhang, X. (2010). DEGseq: an R package for identifying differentially expressed genes from RNA-seq data. *Bioinformatics* 26, 136-138.

53. Chen, C., Chen, H., Zhang, Y., Thomas, H.R., Frank, M.H., He, Y., and Xia, R. (2020). TBtools: an integrative toolkit developed for interactive analyses of big biological data. *Mol Plant* 13, 1194-1202.

54. Wang, N., Yin, Z., Zhao, Y., Wang, J., Pei, Y., Ji, P., Daly, P., Li, Z., Dou, D., and Wei, L. (2022). An F-box protein attenuates fungal xylanase-triggered immunity by destabilizing LRR-RLP NbEIX2 in a SOBIR1-dependent manner. *New Phytol* 236(6):2202-2215.

Acknowledgements

This project has received funding from the National Key Research and Development Plan in the 14th five-year plan (2021YFD1401100: H.J.H, C.X.Z.), National Natural Science Foundation of China (32422075: H.J.H.; U23A6006: J.P.C and C.X.Z.), and the Natural Science Foundation of Zhejiang Province (LDQ24C140001: H.J.H).

Author Contributions Statement

H-JH, J-ML, C-XZ, and J-PC planned and designed the research. XW, J-BL, Y-ZW, H-JH, H-BL, Z-LZ, and Z-XY performed experiments and analyzed data. X-HZ provided the EV plants. H-JH

and XW drafted the manuscript.

Competing Interests Statement

The authors declare no competing interests.

Figure Legends

Fig. 1. BtRDP is a salivary protein and secreted into plants. (**a**) Detection of BtRDP in *Nicotiana tabacum* plants. The untreated and *Bemisia tabaci*-infested tobacco plants are collected for western-blotting assays. Six independent *B. tabaci*-infested plants are tested. The presence of lower intensity band (arrow) in each replicate is summarized in the bracket. Asterisk indicates non-specific binding. Coomassie brilliant blue (CBB) staining is conducted to visualize the sample loading. **(b**, **c)** Detection of BtRDP in different tissues by western-blotting and qRT-PCR assays. Ov, ovary; SG, salivary gland; Ca, carcass; FB, fat body. Silver staining and anti-actin serum are used to visualize the sample loading. (**d**) Expression patterns of BtRDP in different development stages. Ny, nymph; Ps, pseudopupa; Fe, female; Ma, male. *B. tabaci tubulin* is used as an internal control. The relative quantitative method ($2^{-\Delta\Delta Ct}$) is used to evaluate the quantitative variation. Data are presented as mean values ± SEM (n= 3 independent biological replicates). Different lowercase letters indicate statistically significant differences at the $P < 0.05$ level according to one-way ANOVA test followed by Tukey's multiple comparisons test. **(e)** Immunohistochemical staining of BtRDP. The salivary gland and its nearby tissues are dissected and incubate with anti-BtRDP serum or pre-immune serum conjugated with Alexa Fluor™ 488 NHS Ester (green) and actin dye phalloidinrhodamine (red). The nucleus is stained with DAPI (blue). PSG, principal salivary gland; ASG, accessory salivary gland. Experiments are repeated thrice for **(b**), while twice for **(e**). Similar results are observed and representative images are displayed.

Fig. 2. Effects of BtRDP on *Bemisia tabaci*. (**a**) Treating *B. tabaci* with ds*BtRDP* significantly reduces the transcript and protein level of target gene. The ds*GFP*-treated *B. tabaci* is used as a control. qRT-PCR data are presented as mean values ± SEM (n= 6 independent biological replicates). **(b–c)** Effects of *BtRDP* knockdown on insect reproduction **(b)** and feeding behavior **(c)**. Electrical penetration graph (EPG) is used to monitor the insect feeding behavior, which can be classified into nonpenetration (np), pathway duration (C), phloem salivation (E1) and phloem ingestion (E2) phases. All EPG recordings are performed for 8 h. Typical EPG waveforms are displayed in Fig. S8. **(d-f)** Insect performance on transgenic plants overexpressing BtRDP (oeBtRDP). **(d)** Detection of BtRDP in transgenic *Nicotiana tabacum* overexpressing a complete coding region of *BtRDP*. The empty vector (EV) plants are used as the control. The flag tag is fused to the C-terminal ends of

843 recombinant proteins. **(e)** Comparison of insect reproduction on oeBtRDP#1 and EV plants. Five *B.*
844 *tabaci* individuals are confined to indicated plants for 3 days, and the oviposited eggs are counted.
845 **(f)** Attraction of oeBtRDP#1 and EV leaves to *B. tabaci* in a two-choice equipment. A group of 40
846 female *B. tabaci* are released into a device containing oeBtRDP#1 and EV leaves. The number of
847 insects settling on each leaf is counted. After 48 h, the number of eggs on each leaf is counted. **(g-i)**
848 Insect performance on transgenic plants overexpressing BtRDP^{-sp} (oeBtRDP^{-sp}). **(g)** Detection of
849 BtRDP^{-sp} in transgenic *N. tabacum* overexpressing BtRDP without a signal peptide. The insect
850 reproduction **(h)** and settlement **(i)** on oeBtRDP^{-sp} transgenic plants are recorded. Data are presented
851 as mean values ± SEM. The EPG data are first checked for normality and homogeneity of variance,
852 and data not fitting a normal distribution are subjected to log10 transformation. *P*-values are
853 determined by two-tailed unpaired Student's *t* test. ***$P < 0.001$; **$P < 0.01$; *$P < 0.05$; ns, not
854 significant. Western-blotting assays are repeated thrice with the similar results.
855
856 **Fig. 3. NtRLP4 interacts with BtRDP and confers plant resistance to *Bemisia tabaci*. (a)**
857 Domain organization of NtRLP4. NtRLP4 contains a predicted N-terminal signal peptide (SP), a
858 malectin-like domain, a LRR domain, and a transmembrane domain (TM). **(b)** The protein level of
859 NtRLP4 in response to *B. tabaci* infestation. The untreated *Nicotiana tabacum* is used as a negative
860 control. Four independent biological replicates are performed, and the representative images are
861 displayed. The band density is measured using ImageJ. The density values from 4 biological
862 replicates are calculated and the mean value in the controls is set at 1.0. **(c)** Yeast two hybrid assays
863 showing the interaction between BtRDP and NtRLP4. The different combinations of constructs are
864 transformed into yeast cells, and are grown on the selective medium SD/-Trp/-Leu (DDO), and the
865 interactions are tested with SD/-Trp/-Leu/-His/-Ade (QDO). **(d)** Co-immunoprecipitation assay
866 showing the interaction between BtRDP and NtRLP4. Total proteins are extracted from *N.*
867 *benthamiana* leaves transiently co-expressing NtRLP4-myc/NtCf9-myc with BtFTSP-flag/BtRDP-
868 flag. All genes are expressed with a complete coding region, and the myc/flag tags are fused at the
869 C-terminus. Precipitation is performed using flag beads. The samples are probed with anti-flag and
870 anti-myc antibodies for immunoblotting analysis. **(e–h)** Analysis of transgenic *N. tabacum*
871 overexpressing NtRLP4 (oeRLP). **(e)** Detection of NtRLP4 level in oeRLP plants. The empty vector
872 (EV) plant is used as a control. Two independent oeRLP lines are selected. The samples are probed

873 with an anti-NtRLP4 antibody. Rubisco staining (RbcL) is used to visualize the amount of sample
874 loading. **(f)** Attraction of oeRLP#1 and EV leaves to *B. tabaci* in a two-choice equipment. A group
875 of 40 female *B. tabaci* are released into a device containing oeRLP#1 and EV leaves. The number
876 of insects settling on each leaf is counted at each time point. After 48 h, the number of eggs on each
877 leaf is counted. **(g)** Comparison of insect reproduction on oeRLP#1 and EV plants. Five *B. tabaci*
878 individuals are confined to indicated plants for 3 days, and the oviposited eggs are counted. **(h)**
879 Relative transcript levels of salicylic acid (SA)- and jasmonic acid (JA)-associated genes in
880 oeRLP#1 and EV plants. PAL, phenylalanine ammonia lyase; NPR1, nonexpressor of pathogenesis-
881 related protein 1; FAD7, fatty acid desaturase 7; PDF1.2, plant defensin 1.2. Two independent
882 biological replicates are performed in **(d)** and **(e)**. Data in **(f)**, **(g)**, and **(h)** are presented as mean
883 values ± SEM. For insect bioassays in (**f**) and (**g**), n= 10 independent biological replicates. For qRT-
884 PCR in (**h**), n= 3 independent biological replicates. *P*-values are determined by two-tailed unpaired
885 Student's *t* test. ***$P < 0.001$; **$P < 0.01$; *$P < 0.05$; ns, not significant.
886
887 **Fig. 4. BtRDP suppress plant defenses by promoting NtRLP4 degradation. (a)** Effects of
888 ds*BtRDP* suppression on insect reproduction (n= 10 independent biological replicates) when
889 feeding on empty vector (EV) and NtRLP4-silenced (*RNAi-RLP*) transgenic *Nicotiana tabacum*. **(b)**
890 Transient overexpressing BtRDP-mCherry attenuates H_2O_2 accumulation caused by NtRLP4-GFP
891 overexpression. *N. tabacum* co-expressing RFP-mCherry and NtRLP4-GFP is used as a control. All
892 genes are expressed with a complete coding region. The experiment is repeated 5 times with the
893 similar results. **(c)** Relative transcript level of salicylic acid (SA)- and jasmonic acid (JA)-associated
894 genes in BtRDP-mCherry/NtRLP4-GFP and RFP-mCherry/NtRLP4-GFP plants (n=3 independent
895 biological replicates). PAL, phenylalanine ammonia lyase; NPR1, nonexpressor of pathogenesis-
896 related protein 1; FAD7, fatty acid desaturase 7; PDF1.2, plant defensin 1.2. **(d)** Comparison of
897 insect reproduction (n= 16 independent biological replicates) on transient-expressed BtRDP-
898 mCherry/NtRLP4-GFP and RFP-mCherry/NtRLP4-GFP plants. **(e)** Attraction of BtRDP-
899 mCherry/NtRLP4-GFP and RFP-mCherry/NtRLP4-GFP leaves to *B. tabaci* in a two-choice
900 equipment (n= 16 independent biological replicates). The number of eggs on each leaf is counted at
901 48 h post insect release. (**f**) Effects of BtRDP and $BtRDP^{-sp}$ overexpression on NtRLP4
902 accumulation. Transgenic oeBtRDP (left) and $oeBtRDP^{-sp}$ (right) plants are probed with anti-

903 NtRLP4 and anti-flag antibodies for immunoblotting analysis. The experiments are repeated twice
904 with the similar results. **(g)** Degradation of NtRLP4 by BtRDP in *N. benthamiana* leaves. NtRLP4-
905 myc and BtRDP-flag are transiently co-expressed in *N. benthamiana* plants through *Agrobacterium*
906 infiltration. *Agrobacterium* carrying NtCf9-myc and GUS-flag are used as negative controls. **(h)**
907 Effects of 26S proteasome inhibitor (MG132) on NtRLP4 accumulation. Co-infiltrated leaves are
908 treated with MG132 at 24 h post injection. The samples are probed with anti-flag and anti-myc
909 antibodies for immunoblot analysis. Rubisco staining (RbcL) is conducted to visualize the amount
910 of sample loading. The small triangle indicates the different concentrations of *Agrobacterium*
911 (OD_{600} = 0.05, 0.3, and 1.0). **(i)** NtRLP4 is ubiquitinated *in planta*. NtRLP4-myc is co-expressed
912 transiently with HA-UBQ in *N. benthamiana* leaves. Extracted total proteins are
913 immunoprecipitated by anti-myc beads and immunoblotted with anti-myc or anti-HA antibody.
914 Experiments are repeated thrice for (**g**) and (**h**), while twice for **(i**). Band density is measured using
915 ImageJ. The density values from three biological replicates are calculated and the mean value in the
916 first lane is set at 1.0. Data are presented as mean values ± SEM. *P*-values are determined by two-
917 tailed unpaired Student's *t* test. ***$P < 0.001$; **$P < 0.01$; *$P < 0.05$; ns, not significant.
918
919 **Fig. 5. Rice RLP4 are targeted by salivary protein NlSP694 from *Nilaparvata lugens*. (a)**
920 Domain organization of *Oryza sativa* RLP4 (OsRLP4). **(b, c)** Yeast two-hybrid and Co-IP assays
921 showing the interaction between OsRLP4 and NlSP694. All genes are expressed with a complete
922 coding region in Co-IP assays, while NlSP694 without a signal peptide is used in yeast two-hybrid
923 assays. Experiments in (**b**) are repeated twice with the similar result. **(d)** The expression patterns of
924 *NlSP694* in different *N. lugens* tissues. Te, testis; Ov, ovary; SG, salivary gland; Ca, carcass; FB, fat
925 body. Data are presented as mean values ± SEM (n= 3 independent biological replicates). Different
926 lowercase letters indicate statistically significant differences at $P < 0.05$ level according to one-way
927 ANOVA test followed by Tukey's multiple comparisons test. **(e-g)** Effects of dsRNA treatment on
928 insect survivorship (**e**), reproduction (**f**), and honeydew excretion (**g**). For survivorship analysis, a
929 group of 30 *N. lugens* are reared in a cage. Three independent biological replications are performed.
930 Differences in survivorship between the two treatments are tested by log-rank test. ns, not significant.
931 For reproduction analysis, n= 10 and 13 individuals are tested in ds*GFP*- and ds*NlSP694*-treatment,
932 respectively. The sterile females are excluded from data analysis. For honeydew analysis, n= 10

933 independent biological replicates. *P*-values in **(f)** and **(g)** are determined by two-tailed unpaired
934 Student's *t* test. ***$P < 0.001$; **$P < 0.01$. **(h)** Effect of NlSP694 on the accumulation of transient-
935 expressed OsRLP4. OsRLP4-myc is agro-injected into *Nicotiana benthamiana* together with
936 different concentrations of NlSP694-flag and NlSP7-flag. NtCf9-myc is used as a negative control.
937 The small triangle indicates the different concentrations (OD_{600} = 0.05, 0.3, and 1.0) of
938 *Agrobacterium*. Rubisco staining (RbcL) is conducted to visualize the amount of sample loading.
939 Experiments are repeated three times with the similar results. Band density is measured using
940 ImageJ. The density values from three biological replicates are calculated with the mean value in
941 the first lane being set at 1.0.
942
943 **Fig. 6. The proposed model for the suppression of receptor-like proteins (RLPs)-mediated**
944 **plant defenses by salivary effectors.** Host plants employ pattern-recognition receptors (PRRs) to
945 detect various damage-associated molecular patterns (DAMPs) and herbivore-associated molecular
946 patterns (HAMPs) triggered by insect feeding. The RLP4/SOBIR1 complex plays a vital role in
947 initiating pattern-triggered immunity (PTI), including H_2O_2 burst, upregulation of jasmonic acid
948 (JA), and downregulation of salicylic acid (SA), which hinders insect feeding. The whitefly *Bemisia*
949 *tabaci* and planthopper *Nilaparvata lugens* independently evolved salivary proteins that targeted
950 plant RLP4. *B. tabaci* salivary sheath protein BtRDP interacts with the leucine-rich repeat (LRR)
951 domain of RLP4 from *Nicotiana tabaci* and *Solanum lycopersicum*, while *N. lugens* NlSP694 targets
952 both the LRR domain and the malectin-like domain of *Oryza sativa* RLP4. These interactions
953 promote the ubiquitin-dependent degradation of RLP4, thereby disrupting the stability of the
954 RLP4/SOBIR1 complex. The presence of salivary effectors causes a hormonal shift and suppresses
955 the H_2O_2 burst, finally favoring insect feeding.

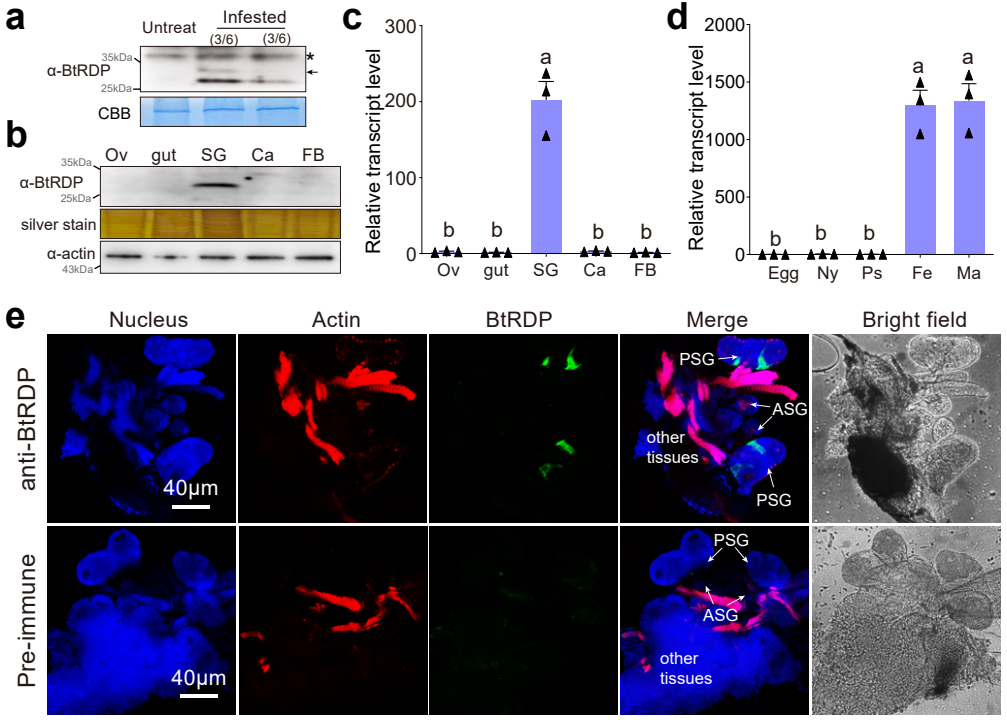
a
Untreat
Infested
(3/6)
(3/6)
35kDa
α-BtRDP
25kDa
CBB
b
Ov
gut
SG
Ca
FB
35kDa
α-BtRDP
25kDa
silver stain
α-actin
43kDa
c
Relative transcript level
300
200
100
0
a
b
b
b
b
Ov
gut
SG
Ca
FB
d
Relative transcript level
2000
1500
1000
500
0
a
a
b
b
b
Egg
Ny
Ps
Fe
Ma
e
Nucleus
Actin
BtRDP
Merge
Bright field
anti-BtRDP
Pre-immune
40μm
40μm
PSG
ASG
other tissues
PSG
PSG
ASG
other tissues

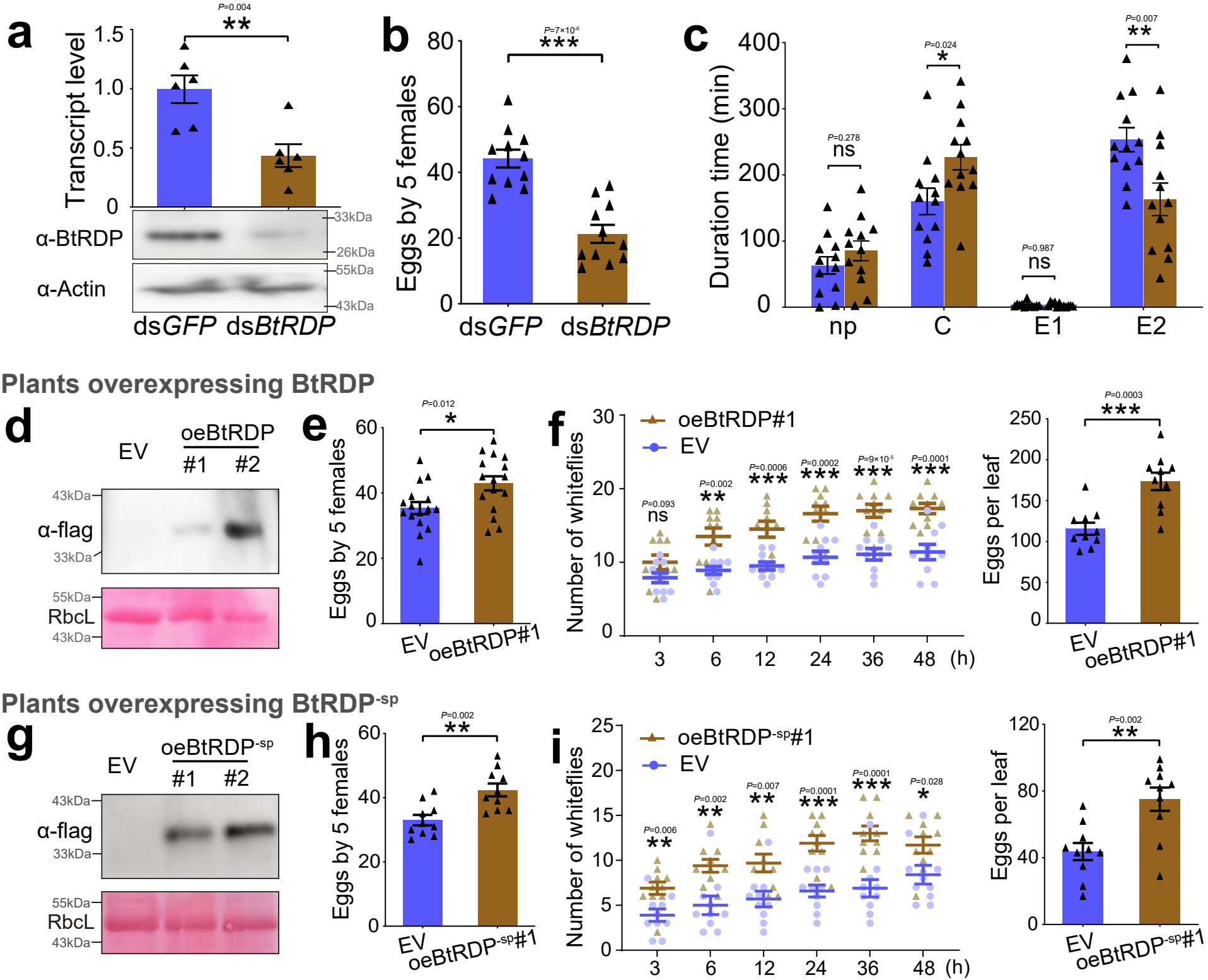
a
Transcript level
P=0.004
**
α-BtRDP
α-Actin
33kDa
26kDa
55kDa
43kDa
dsGFP dsBtRDP
b
Eggs by 5 females
P=7×10-6
***
dsGFP dsBtRDP
c
Duration time (min)
P=0.278
ns
P=0.024
*
P=0.987
ns
P=0.007
**
np
C
E1
E2
Plants overexpressing BtRDP
d
EV
oeBtRDP
#1 #2
α-flag
RbcL
e
Eggs by 5 females
P=0.012
*
EV oeBtRDP#1
f
Number of whiteflies
oeBtRDP#1
EV
P=0.093 ns
P=0.002 **
P=0.0006 ***
P=0.0002 ***
P=9×10-5 ***
P=0.0001 ***
3 6 12 24 36 48 (h)
Eggs per leaf
P=0.0003
***
EV oeBtRDP#1
Plants overexpressing BtRDP-sp
g
EV
oeBtRDP-sp
#1 #2
α-flag
RbcL
h
Eggs by 5 females
P=0.002
**
EV oeBtRDP-sp#1
i
Number of whiteflies
oeBtRDP-sp#1
EV
P=0.006 **
P=0.002 **
P=0.007 **
P=0.0001 ***
P=0.0001 ***
P=0.028 *
3 6 12 24 36 48 (h)
Eggs per leaf
P=0.002
**
EV oeBtRDP-sp#1

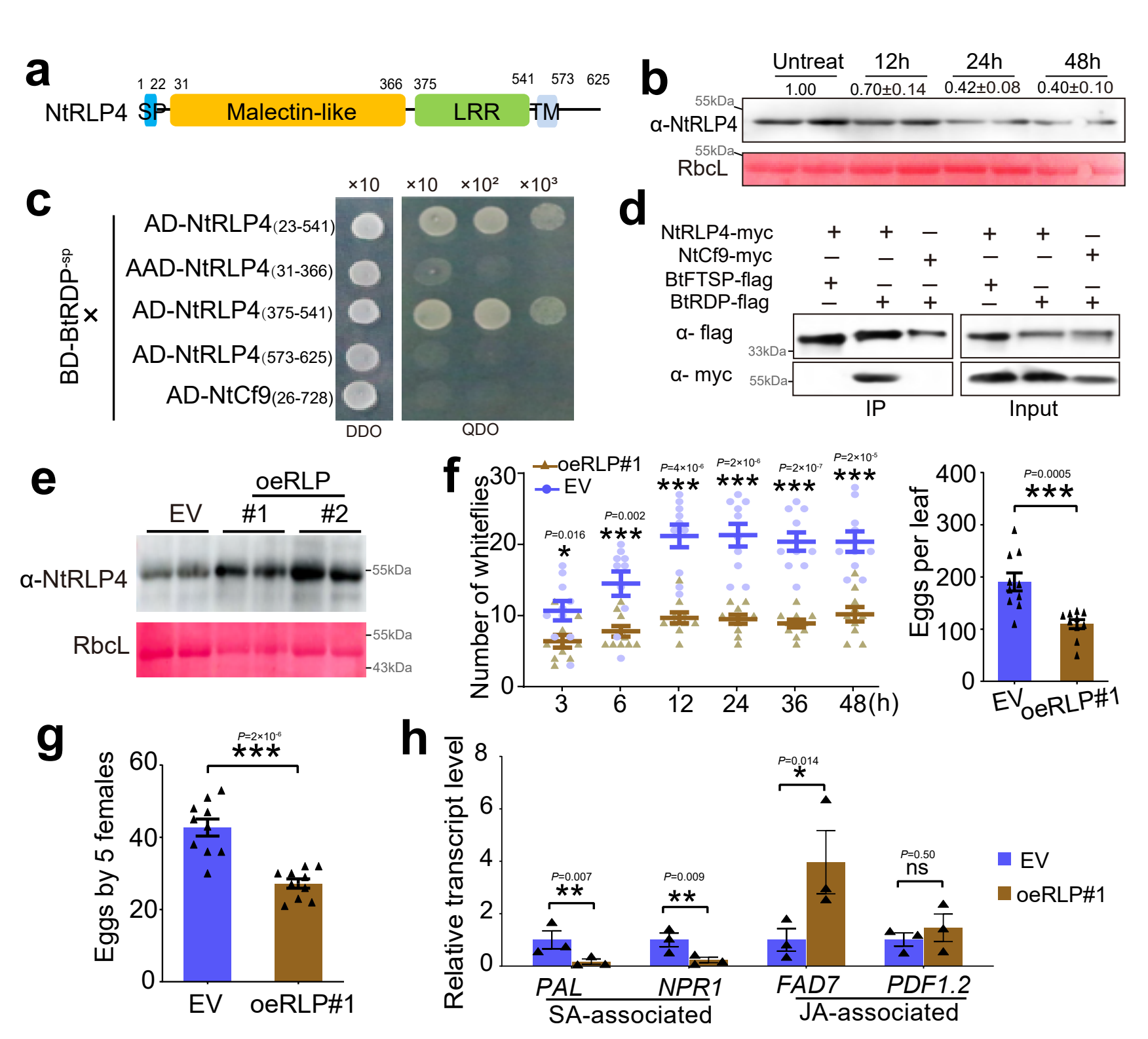
a
NtRLP4
1 22 31
SP
Malectin-like
366 375
LRR
541 573 625
TM
b
Untreat
12h
24h
48h
1.00
0.70±0.14
0.42±0.08
0.40±0.10
55kDa
α-NtRLP4
55kDa
RbcL
c
BD-BtRDP-sp
×
AD-NtRLP4(23-541)
AAD-NtRLP4(31-366)
AD-NtRLP4(375-541)
AD-NtRLP4(573-625)
AD-NtCf9(26-728)
×10
×10
×10²
×10³
DDO
QDO
d
NtRLP4-myc
NtCf9-myc
BtFTSP-flag
BtRDP-flag
α- flag
33kDa
α- myc
55kDa
IP
Input
e
EV
oeRLP
#1
#2
α-NtRLP4
55kDa
RbcL
55kDa
43kDa
f
oeRLP#1
EV
Number of whiteflies
P=0.016
P=0.002
P=4×10⁻⁶
P=2×10⁻⁶
P=2×10⁻⁷
P=2×10⁻⁵
3
6
12
24
36
48(h)
Eggs per leaf
P=0.0005
EV
oeRLP#1
g
Eggs by 5 females
P=2×10⁻⁶
EV
oeRLP#1
h
Relative transcript level
P=0.007
P=0.009
P=0.014
P=0.50
ns
PAL
NPR1
FAD7
PDF1.2
SA-associated
JA-associated
EV
oeRLP#1

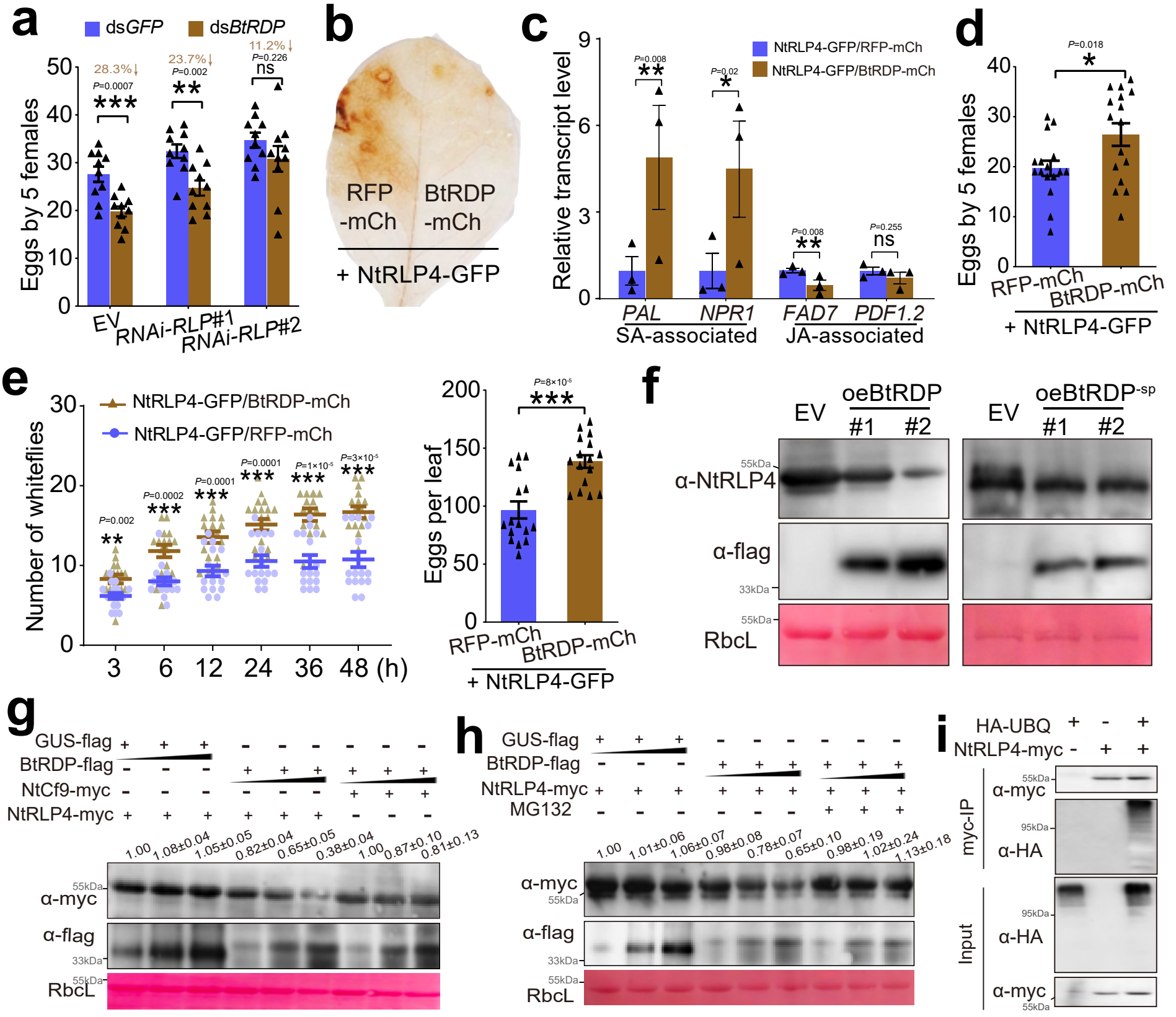
a
dsGFP
dsBtRDP
Eggs by 5 females
28.3%↓
23.7%↓
11.2%↓
P=0.0007
P=0.002
P=0.226
***
**
ns
EV
RNAi-RLP#1
RNAi-RLP#2
b
RFP -mCh
BtRDP -mCh
+ NtRLP4-GFP
c
NtRLP4-GFP/RFP-mCh
NtRLP4-GFP/BtRDP-mCh
Relative transcript level
P=0.008
P=0.02
P=0.008
P=0.255
PAL
NPR1
FAD7
PDF1.2
SA-associated
JA-associated
d
P=0.018
Eggs by 5 females
RFP-mCh
BtRDP-mCh
+ NtRLP4-GFP
e
NtRLP4-GFP/BtRDP-mCh
NtRLP4-GFP/RFP-mCh
Number of whiteflies
P=0.002
P=0.0002
P=0.0001
P=0.0001
P=1×10-5
P=3×10-5
3
6
12
24
36
48 (h)
Eggs per leaf
P=8×10-5
RFP-mCh
BtRDP-mCh
+ NtRLP4-GFP
f
EV
oeBtRDP
#1
#2
EV
oeBtRDP-sp
#1
#2
55kDa
α-NtRLP4
α-flag
33kDa
55kDa
RbcL
g
GUS-flag
BtRDP-flag
NtCf9-myc
NtRLP4-myc
1.00
1.08±0.04
1.05±0.05
0.82±0.04
0.65±0.05
0.38±0.04
1.00
0.87±0.10
0.81±0.13
55kDa
α-myc
α-flag
33kDa
55kDa
RbcL
h
GUS-flag
BtRDP-flag
NtRLP4-myc
MG132
1.00
1.01±0.06
1.06±0.07
0.98±0.08
0.78±0.07
0.65±0.10
0.98±0.19
1.02±0.24
1.13±0.18
α-myc
55kDa
α-flag
33kDa
55kDa
RbcL
i
HA-UBQ
NtRLP4-myc
55kDa
α-myc
95kDa
α-HA
myc-IP
95kDa
α-HA
Input
α-myc
55kDa

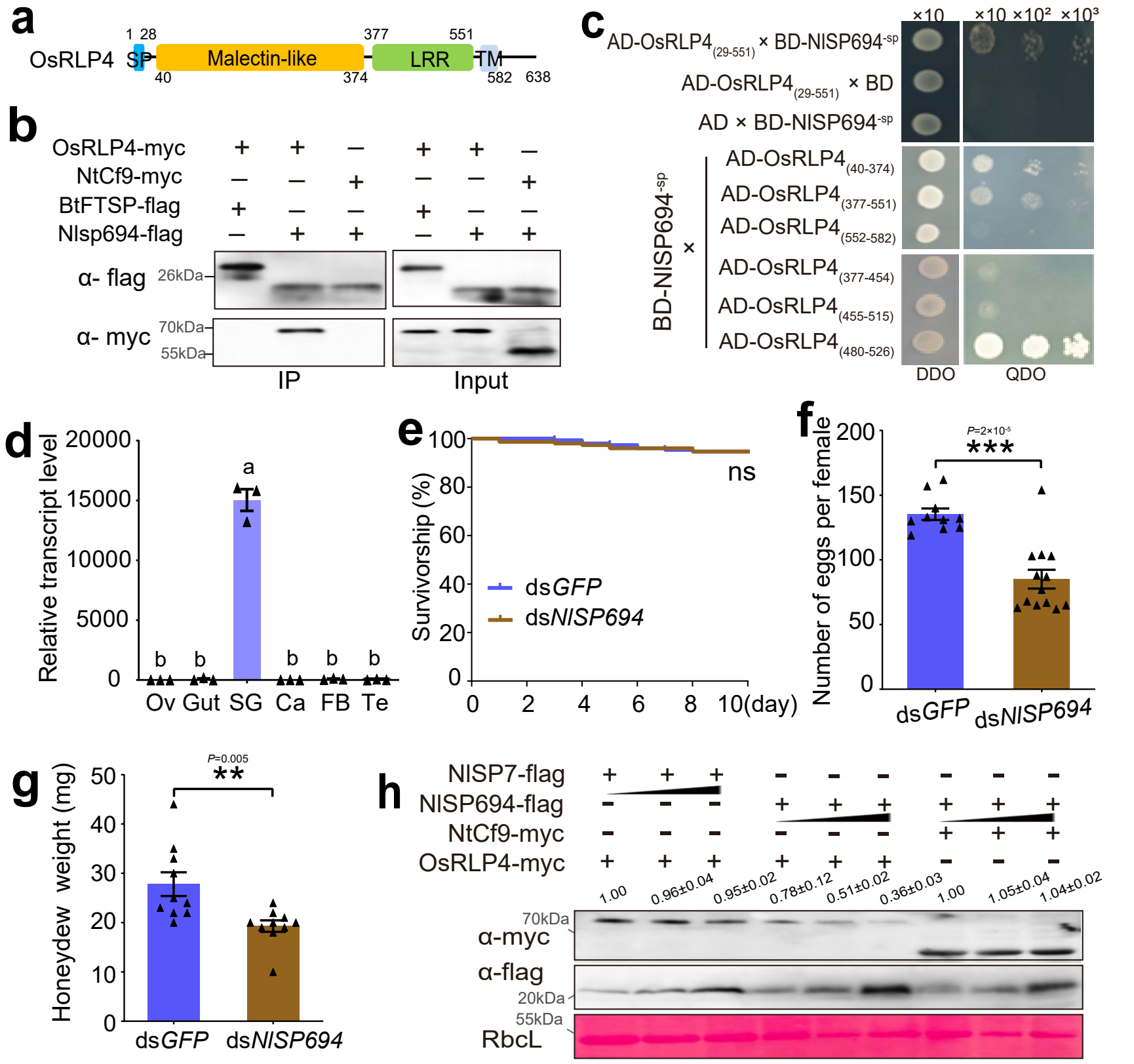
a
OsRLP4
SP
Malectin-like
LRR
TM
1 28
40
377
374
551
582
638
b
OsRLP4-myc
NtCf9-myc
BtFTSP-flag
Nlsp694-flag
α- flag
α- myc
26kDa
70kDa
55kDa
IP
Input
c
AD-OsRLP4(29-551) × BD-NISP694-sp
AD-OsRLP4(29-551) × BD
AD × BD-NISP694-sp
BD-NISP694-sp
AD-OsRLP4(40-374)
AD-OsRLP4(377-551)
AD-OsRLP4(552-582)
AD-OsRLP4(377-454)
AD-OsRLP4(455-515)
AD-OsRLP4(480-526)
×10
×10 ×10² ×10³
DDO
QDO
d
Relative transcript level
Ov Gut SG Ca FB Te
e
Survivorship (%)
ns
dsGFP
dsNISP694
10(day)
f
Number of eggs per female
P=2×10-5
***
dsGFP
dsNISP694
g
Honeydew weight (mg)
P=0.005
**
dsGFP
dsNISP694
h
NISP7-flag
NISP694-flag
NtCf9-myc
OsRLP4-myc
1.00
0.96±0.04
0.95±0.02
0.78±0.12
0.51±0.02
0.36±0.03
1.00
1.05±0.04
1.04±0.02
70kDa
α-myc
α-flag
20kDa
55kDa
RbcL

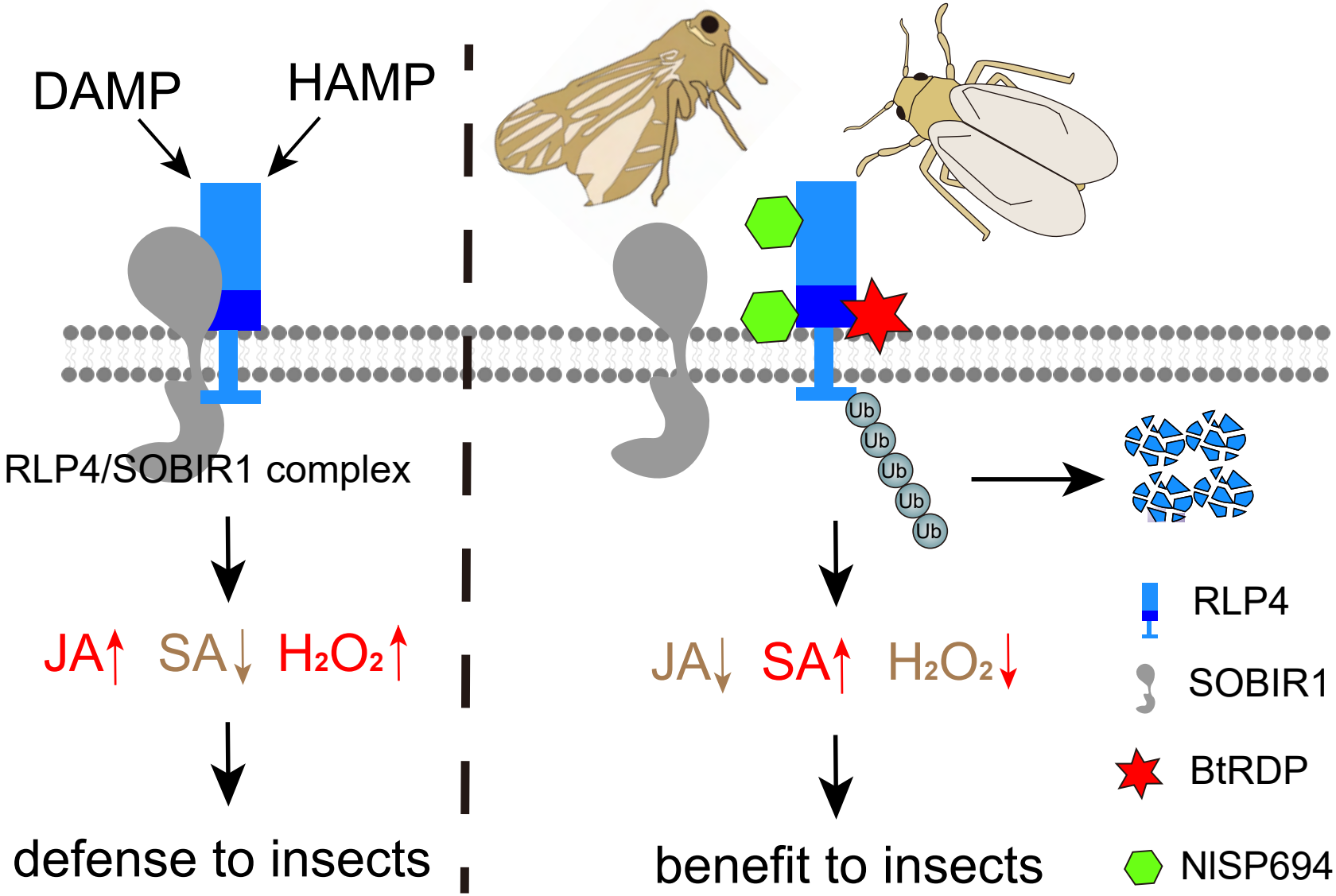
DAMP
HAMP
RLP4/SOBIR1 complex
JA↑ SA↓ H2O2↑
defense to insects
Ub
JA↓ SA↑ H2O2↓
benefit to insects
RLP4
SOBIR1
BtRDP
NISP694